

Immunogenicity of non-canonical HLA-I tumor ligands identified through proteogenomics

Authors

Maria Lozano-Rabella¹, Andrea Garcia-Garijo¹, Jara Palomero¹, Anna Yuste-Estevanez¹, Florian Erhard², Juan Martín-Liberal³, Maria Ochoa de Olza³, Ignacio Matos³, Jared J. Gartner⁴, Michael Ghosh⁵, Francesc Canals⁶, August Vidal⁷, Josep Maria Piulats⁸, Xavier Matias-Guiu⁷, Irene Braña³, Eva Muñoz-Couselo⁹, Elena Garralda³, Andreas Schlosser², Alena Gros¹

Affiliations:

1 Tumor Immunology and Immunotherapy, Vall d'Hebron Institute of Oncology (VHIO), Vall d'Hebron Barcelona Hospital, Barcelona, Spain

2 Rudolf Virchow Center, Center for Integrative and Translational Bioimaging, Julius-Maximilians-University Würzburg, Germany

3 Early Drug Development Unit (UITM) Vall d'Hebron Institute of Oncology (VHIO), Vall d'Hebron Barcelona Hospital, Barcelona, Spain

4 Surgery Branch, National Cancer Institute (NCI), National Institutes of Health, Bethesda, Maryland, USA

5 Institute for Cell Biology Department of Immunology, University of Tübingen, Germany

6 Proteomics, Vall d'Hebron Institute of Oncology (VHIO), Vall d'Hebron Barcelona Hospital, Barcelona, Spain

7 Department of Pathology. Hospital Universitari de Bellvitge-IDIBELL. CIBERONC

8 Medical Oncology, Catalan Institute of Cancer (ICO), IDIBELL-Oncobell, Hospitalet de Llobregat, Spain

9 Melanoma and other skin tumors unit, Vall d'Hebron Institute of Oncology (VHIO), Vall d'Hebron Barcelona Hospital

Corresponding Author:

Alena Gros

Email: agros@vhio.net

Address: c/ Natzaret 115-117, Cellex Center Lab 4.04A, 08035 Barcelona, Spain

Conflict-of-interest statement

A.G. is member of the scientific advisory board (SAB) of Achilles Therapeutics plc, SingulaBIO, RootPath, Inc., and BioNTech SE, and consults for PACT Pharma, Inc., and Instil Bio. AG is co-inventor of patents licensed and with royalties E-059-2013/0 E-085-2013/0, E-149-2015/0. J.M.L. has received lecture fees from Astellas, Bristol-Myers Squibb, MSD, Novartis, Pierre Fabre, Pfizer, Roche, Sanofi; advisory fees from Bristol-Myers Squibb, Highlight Therapeutics, Novartis, Pierre Fabre, Roche, Sanofi; research grants from Sanofi; and travel grants from Bristol-Myers Squibb, MSD, Novartis, Pierre Fabre, Pfizer, Roche, Ipsen. E. M. is a member of the advisory board of Amgen, Bristol-Myers Squibb, Merck Sharp & Dohme, Novartis, Pierre Fabre, Roche, Sanofi. Honoraria: Amgen, Bristol-Myers Squibb, Merck Sharp & Dohme, Novartis, Pierre Fabre, Roche. Clinical trial participation (principal investigator): Amgen, Bristol-Myers Squibb, GlaxoSmithKline, Merck Sharp & Dohme, Novartis, Pierre Fabre, Roche, Sanofi. J.M.P is consultant for IMMUNOCORE, MSD, BMS, Roche. J.M.P has received research grants from BeiGene, MSD, BMS, Pfizer and Janssen. E.G. is a consultant advisor of Roche/Genentech, F.Hoffmann/La Roche, Ellipses Pharma, Neomed Therapeutics1 Inc, Boehringer Ingelheim, Janssen Global Services, SeaGen, TFS, Alkermes, Thermo Fisher-Bristol-Mayers Squibb, MabDiscovery, Anaveon, F-Star Therapeutics, Hengrui. Remaining authors declare that no other conflict of interest exists.

44 **Statement of translational relevance**

45 Recent evidence suggests that peptides derived from non-canonical aberrantly translated proteins
46 can be presented on HLA-I by tumor cells, but detailed studies of their immunogenicity are lacking. Our
47 findings provide key insights for the clinical exploitation of non-canonical HLA-I ligands as targets for
48 vaccines or T-cell therapies. We found that peptides derived from non-canonical proteins were frequently
49 presented on HLA-I of patient-derived tumor cell lines (TCL) across different tumor types. Unlike
50 neoantigens, CG or melanocyte differentiation antigens, non-canonical HLA-I ligands did not frequently
51 elicit antitumor T-cell responses in cancer patients, suggesting they play a limited role in immune
52 surveillance and immune-editing. However, in vitro raised T-cell responses and TCRs targeting 3 non-
53 canonical peptides recognized their specific antigens naturally presented by tumor cells, targeted multiple
54 TCL and did not or barely target normal cells tested. These findings support that specific non-canonical HLA-
55 I peptides may represent valuable targets for widely applicable immunotherapies.

56

57

58

59

60

61

62

63

64

65

66

67

68

69

70

71

72

73

74

75

76

77

78 **Abstract**

79 Tumor antigens are central to antitumor immunity. Recent evidence suggests that peptides from
80 non-canonical (nonC) aberrantly translated proteins can be presented on HLA-I by tumor cells. Here, we
81 investigated the immunogenicity of nonC tumor HLA-I ligands (nonC-TL) to better understand their
82 contribution to cancer immunosurveillance and their therapeutic applicability. Using proteogenomics, we
83 identified 517 nonC-TL from 9 patients with melanoma, gynecological, and head and neck cancer. We found
84 no recognition of the 507 nonC-TL tested by autologous *ex vivo* expanded tumor reactive T-cell cultures
85 while the same cultures demonstrated reactivity to mutated, cancer-germline, or melanocyte
86 differentiation antigens. However, *in vitro* sensitization of donor peripheral blood lymphocytes against 170
87 selected nonC-TL, led to the identification of T-cell receptors (TCRs) specific to three nonC-TL, two of which
88 mapped to the 5' UTR regions of HOXC13 and ZKSCAN1, and one mapping to a non-coding spliced variant of
89 C5orf22C. T cells targeting these nonC-TL recognized cancer cell lines naturally presenting their
90 corresponding antigens. Expression of the three immunogenic nonC-TL was shared across tumor types and
91 barely or not detected in normal cells. Our findings predict a limited contribution of nonC-TL to cancer
92 immunosurveillance but demonstrate they may be attractive novel targets for widely applicable
93 immunotherapies.

94 **Introduction**

95 Tumor antigens are central to antitumor immunity. Peptides derived from tumor antigens presented
96 on HLA molecules (pHLA) on the surface of cancer cells can elicit protective and therapeutic T-cell
97 responses(1). The existence of T cells targeting non-mutated tumor-associated antigens (TAA) and cancer-
98 germline antigens (CGA) in cancer patients is well established(2,3). Their shared expression in a substantial
99 fraction of tumors has led to the development of widely applicable vaccines or T cell-based therapies (4,5).
100 However, off-tumor toxicities have been reported(6–8). Technological advances in next-generation
101 sequencing (NGS) and tandem mass spectrometry coupled with high-throughput immunological and HLA
102 multimer screens have expedited the systematic discovery of the personalized landscape of antigens
103 contributing to tumor immunogenicity. Accumulating evidence demonstrates that neoantigens arising from
104 non-synonymous somatic mutations (NSM) greatly contribute to the immunogenicity of human tumors. For
105 instance, neoantigen-specific T cells are frequently detected in cancer patients (9–13) and mutational load
106 correlates with the clinical benefit of immune checkpoint blockade (ICB)(14). Their foreign nature and high
107 tumor specificity together with the antitumor responses observed following transfer of neoantigen-specific
108 T cells in selected patients (15–18) render these attractive targets. Yet, existing techniques still fail to
109 capture most antigens targeted by tumor-reactive T cells and this constitute a major obstacle for the
110 development of immunotherapy.

111 Tumor antigen discovery efforts thus far have largely investigated the immunogenicity of selected
112 genomically annotated proteins or NSM in coding regions, limited to only 2% of the genome. However, up
113 to 75% of the genome can be transcribed and, potentially, translated(19). Emerging data demonstrate that
114 peptides derived from alternative open reading frames (ORF) or from allegedly non-coding regions referred
115 to as non-canonical (nonC) or cryptic antigens are frequently presented on HLA-I molecules (20–23). A
116 fraction of such aberrant translation events has been postulated to be specifically presented on tumor cells,
117 thus substantially expanding the repertoire of targetable tumor antigens (24–27). Their non-mutated
118 nature and occasional shared presentation across different tumors, has further attracted attention to nonC
119 proteins as targets for immunotherapy.

120 Despite the potential of tumor-specific nonC HLA-I ligands as a source of tumor antigens, their
121 systematic identification in humans remains challenging. Spontaneous T-cell responses against peptides
122 derived from nonC proteins have been rarely identified using cumbersome and time-consuming
123 immunological screens of tumor cDNA libraries (28–30). A growing number of recent studies have exploited
124 immunopeptidomics to identify these antigens (22–27,31), but their immunogenicity and their selective
125 expression in cancer remains largely unexplored. Here, we investigated the presentation and
126 immunogenicity of nonC antigens across different cancer types to better understand their contribution to
127 cancer immunosurveillance and to address their therapeutic potential. We employed a proteogenomics
128 pipeline(20) to identify nonC HLA-I ligands derived from off-frame translation of coding sequences and non-
129 coding regions (UTR, ncRNA, intronic and intergenic) in patient-derived tumor cell lines (TCLs) of different
130 histological types. We further modified the pipeline to select peptides preferentially presented by cancer
131 cells and evaluated their natural or induced immunogenicity by assessing pre-existing and *in vitro*-sensitized
132 T-cell responses.

133 **Results**

134 **Non-canonical tumor HLA-I ligands are frequently identified in patient-derived tumor cell lines**

135 We first sought to determine whether tumor-specific nonC HLA-I ligands could be identified in 9
136 short-term cultured TCL derived from four gynecological cancer (Gyn), three melanoma (Mel) and two head
137 and neck (H&N) cancer patients (Supplemental Table 1). These samples were selected irrespective of the
138 tumor histology, solely based on the availability of matched *ex vivo* expanded TIL and/or peripheral blood
139 tumor-reactive lymphocyte populations.

140 To this end, peptides bound to HLA-I were isolated and analyzed by liquid chromatography coupled
141 to tandem mass spectrometry (LC-MS/MS) using state-of-the-art procedures. Amino acid (Aa) sequences
142 were identified through a previously described pipeline, Peptide-PRISM(20), with some modifications
143 (Figure 1A). Briefly, for each MS spectrum, the top 10 candidates were first identified by *de novo*
144 sequencing and later mapped to a database including the 3-frame transcriptome and 6-frame genome.
145 Additionally, whole-exome sequencing (WES) information of each TCL was included to interrogate the
146 presentation of mutated peptides derived from cancer-specific NSM. The false-discovery rate (FDR) was
147 calculated independently for each category considering the search space and peptide length in a stratified
148 mixture model as previously described (20). Following this strategy and selecting a 1% FDR, we identified
149 839 nonC peptides presented on HLA-I in all the TCLs studied, ranging from 0.5% to 5.4% of the total eluted
150 peptides (Figure 1B).

151 In order to select nonC peptides preferentially presented by tumor cells, immunopeptidomics data
152 from samples available from the HLA ligand atlas (32) was used to filter out peptides known to be
153 presented in healthy tissues (Figure 1A). Although LC-MS/MS is less sensitive than RNA-seq, this technique
154 is capable of capturing canonical as well as aberrant translation. Given that we leveraged an
155 immunopeptidomics database derived from donors presenting a fraction of all potential HLA alleles, nonC
156 peptides were excluded at the ORF level rather than the Aa sequence to overcome a potential bias toward
157 frequent alleles. As a result, we found that from a total of 839 unique nonC peptides detected in our tumor
158 samples, 322 (38.38%) were predicted to derive from ORFs also present in healthy tissue (nonC-HL). Hence,
159 517 (61.6%) were considered preferentially presented on tumor HLA-I and referred to as non-canonical
160 tumor ligands (nonC-TL) (Figure 1C). NonC-TL displayed similar characteristics as peptides derived from
161 canonical proteins such as the MS identification score (ALC) or the correlation of the retention time with
162 the hydrophobicity index (Figure 1D and 1E). Additionally, nonC-TL exhibited expected HLA-I ligand features
163 as shown by the length distribution ranging from 8-12 Aa and the high percentage of peptides predicted to
164 bind to the patient's HLA alleles according to NetMHCpan4.0 (Figure 1F and 1G). Moreover, as with the
165 HLA-I peptides derived from canonical proteins, most of the nonC-TL were validated by MS using synthetic
166 or isotope labeled peptides, (Supplemental Figure 1-2). Altogether, these analyses indicate that our
167 approach accurately identified the HLA-I ligand repertoire including nonC-TL presented by patient-derived
168 TCL.

169 Next, we evaluated the genomic origin of the identified nonC-TL. Consistent with previous studies
170 (20,33,34), we found that translation of 5'UTR was the main origin followed by off-frame and non-coding
171 RNA (ncRNA) (Figure 1H). Peptides derived from 3'UTR, intronic and intergenic regions were less frequently
172 detected. In addition, one nonC peptide derived from a 5'UTR containing a tumor-specific mutation was
173 detected in patient Gyn-3 (Figure 1H). We noticed a clear bias in the HLA-I binding preference distribution
174 of nonC ligands towards HLA-A*11:01 and HLA-A*03:01 alleles according to NetMHCpan4.0 (Figure 1I and
175 Supplemental Figure 3). Both HLA alleles bind peptides with a similar motif containing basic residues at p9

176 (Figure 1J), a unique feature among all the alleles studied (Supplemental Figure 4). Indeed, the binding
177 preference of nonC peptides to both HLA-A*11:01 and HLA-A*03:01 alleles has been previously reported in
178 other immunopeptidomics studies (20,21), however the exact mechanism underpinning this bias is still
179 unknown. Overall, our results showed that nonC-TL are frequently detected in patient-derived TCLs.
180 Importantly, 76 of our nonC-TL were found in published HLA-I immunopeptidomics datasets from
181 melanoma resection samples (35,36) (Supplemental Figure 5), supporting that HLA-I presentation of nonC-
182 TL is not an artifact of *in vitro* cultured cells and that these peptides can be naturally presented *in vivo*.

183 **NonC-TL constitute an abundant source of candidate tumor antigens**

184 To examine whether nonC-TL represent an attractive source of tumor antigens that could be
185 exploited therapeutically we first compared the number of nonC-TL eluted from HLA-I to those derived
186 from conventional tumor antigen sources, including peptides encoded by canonical coding regions derived
187 from somatically mutated gene products, and from TAA such as CGA or melanoma-associated antigens
188 arising from melanocyte differentiation proteins. While the number of HLA-I ligands derived from canonical
189 tumor antigens ranged from 24 to 36 peptides, nonC-TL outnumbered the other categories, with 517
190 unique tumor antigen candidates in all the TCL studied (Figure 2A). Of note, this observation was consistent
191 across most of the patients studied (Figure 2B). In more detail, a total of 33 mutated peptides were
192 detected in 6 out of 9 patients. Despite the number of eluted HLA-I ligands containing mutations was low
193 compared to the total NSM identified by WES, these results are in line with previous immunopeptidomics
194 studies where few mutations are typically detected(36–38) (Figure 2B and 2C). Moreover, 36 peptides
195 derived from 12 genes encoding for CGA and 24 peptides derived from 5 melanoma-associated antigens
196 were identified in 8 out of 9 patients (Figure 2D). Furthermore, nonC-TL mainly originated from 5'UTR and
197 off-frame translation in most patients, while peptides derived from intergenic and intronic regions were not
198 or barely detected (Figure 2E).

199 One advantage of exploiting non-mutated antigens over private mutations as targetable tumor
200 antigens is the fact that they can be shared across patients, which could facilitate the development of off-
201 the-shelf vaccines or T-cell-based therapies. Similar to CGA or melanoma-associated antigens, we observed
202 that ~10% of nonC-TL were shared among at least 2 patients (Figure 2F). In contrast, all mutated HLA-I
203 ligands detected were derived from private mutations and thus, exclusively identified in a single patient. Of
204 note, nonC-TL showed the highest number of shared peptides, including one and three sequences
205 identified in 5 and 4 patients, respectively (Figure 2F). Altogether, this data highlights nonC-TL as promising
206 targets for the development of therapeutic interventions since they constitute a broader spectrum of
207 candidate tumor antigens compared to peptides derived from mutations, CGA, or melanoma-associated
208 antigens and can be shared across patients.

209 **Tumor-reactive T cells in cancer patients preferentially recognize neoantigens and TAA rather 210 than nonC-TL**

211 To further evaluate the role of nonC-TL in cancer immunosurveillance we assessed the presence of
212 spontaneous T-cell responses targeting personalized candidate tumor antigens including nonC-TL, mutated,
213 CGA and melanoma-associated antigens in the nine cancer patients. To this end, *ex vivo* expanded tumor-
214 infiltrating (TIL) or peripheral blood lymphocyte (PBL) populations reactive to their corresponding
215 autologous TCL were co-cultured with autologous antigen presenting cells (APC) pulsed with the synthetic
216 peptides encoding the candidate antigens identified through proteogenomics. T-cell reactivity was tested
217 by IFN- γ release and the upregulation of the activation cell-surface marker 4-1BB assessed by ELISPOT and
218 flow cytometry, respectively (Figure 3A, 3B, and Supplemental Figure 6).

219 In patient Mel-3, we detected T-cell reactivity to at least one candidate peptide in 5 out of 11
220 different tumor-reactive TIL populations interrogated. TILs recognized two neoantigens (ETV1_{p.E455K} and
221 GEMIN5_{p.S1360L}) and two immunogenic peptides derived from melanoma-associated antigens (PMEL and
222 MLANA). However, no reactivity was detected to any of the 9 peptides derived from CGA nor the 215 nonC-
223 TL tested (Figure 3A). To further confirm and characterize the T-cell responses observed, antigen-specific T
224 cells were enriched by flow cytometry based-sorting of 4-1BB⁺ cells followed by *ex vivo* expansion (Figure
225 3C). The neoantigen-specific enriched populations showed a higher response to the mutated peptide than
226 to the wild type (Wt) counterparts as shown by peptide titration experiments, although T cells exhibited a
227 variable functional avidity to their cognate antigen (Figure 3D). ETV1_{p.E455K} and GEMIN5_{p.S1360L} were
228 restricted to HLA-B*35:01 and HLA-A*11:01, respectively (Figure 3E). Importantly, co-culture experiments
229 showed that both neoantigen-specific T cells isolated recognized the autologous TCL, ultimately
230 demonstrating that these peptides are naturally processed and presented by the tumor (Figure 3C and 3E).

231 We used the same strategy to identify and characterize pre-existing T-cell responses targeting
232 candidate tumor antigens from all patients included in the study (Figure 3F). In total, screening of pre-
233 existing tumor-reactive T cells for recognition of 600 tumor antigen candidates led to the detection of 20
234 immunogenic peptides in the 9 cancer patients studied (Figure 3F; Table 1). Of note, we could detect T-cell
235 responses to at least one neoantigen in the six patients in which neoantigen candidates were detected
236 through immunopeptidomics. Overall, 13 out of the 33 mutated HLA-I ligands tested were immunogenic,
237 representing 39% of the total neoantigen candidates. Furthermore, four immunogenic peptides derived
238 from CGA and three derived from melanoma-associated antigens were also recognized by naturally
239 occurring tumor-reactive T cells. A detailed characterization of the antigen-specific T cells isolated including
240 autologous tumor recognition, HLA restriction, functional avidity and Wt counterpart recognition for
241 neoantigens is shown in Supplemental Figure 7-10. In contrast, none of the 507 unique nonC-TL candidates
242 interrogated were able to elicit a recall immune response in any of the studied patients. Altogether, these
243 results reveal that although nonC-TL were frequently detected in TCL, antigens derived from canonical
244 regions were preferentially recognized by tumor-reactive lymphocytes.

245 **NonC-TL recognized by *in vitro* sensitized T cells are shared across patient-derived TCL**

246 Although we did not detect pre-existing T-cell responses targeting nonC-TL, we reasoned that these
247 antigens could still be immunogenic, and thus could represent attractive targets for T-cell therapies or
248 vaccines. To address this question, we investigated the presence of naïve T cells specific to nonC-TL- in the
249 repertoire of healthy individuals carrying the corresponding HLA restriction alleles. As such peptide specific
250 TCR are in very low frequency we sought to enrich nonC-TL-specific T cells through *in vitro* sensitization
251 (IVS) in a non-autologous HLA-matched setting (Figure 4A).

252 Out of the total 507 nonC-TL identified in all patients, we selected 170 peptides predicted to bind to
253 HLA-A*11:01 according to NetMHCpan4.0, an allele expressed in 14% of the Caucasian population
254 (<http://allelefrequencies.net>). Through IVS of PBL from an HLA-A*11:01 donor, we detected, isolated, and
255 expanded T cells specifically recognizing three nonC-TL (Figure 4B). Two peptides mapped to 5'-UTR regions
256 of the canonical genes HOXC13 (5'-U-HOXC13) and ZKSCAN1 (5'-U-ZKSCAN1), and one peptide mapped to a
257 non-coding spliced variant of C5orf22C gene (nc-C5orf22C, Supplemental Figure 11). The ORF encoding
258 these nonC-TL were considerably short, with up to 21, 46, or 49 amino acids respectively, as confirmed by
259 the recognition of APC electroporated with RNA encoding the predicted ORF (Supplemental Figure 12).
260 Additionally, the loss of recognition of TCL transduced with Cas9-sgRNA targeting the 5'UTR HOXC13
261 genomic locus unequivocally confirmed the specificity of the T cells for this antigen and the exact genomic
262 location from which it is transcribed and translated (Supplemental Figure 13).

263 Although these three immunogenic nonC-TL were originally detected in Mel-3 TCL through
264 immunopeptidomics, we investigated whether these antigens could be also expressed in other tumor cell
265 lines. We exploited the high sensitivity of the nonC antigen-specific T cells identified to evaluate the
266 expression and translation of these nonC antigens in a panel of 24 patient-derived TCL. T cells were co-
267 cultured with TCL artificially expressing the restriction element of interest (i.e., HLA-A*11:01 for 5'U-
268 HOXC13 and nc-C5orf22, and HLA-A*68:01 for 5'U-ZKSCAN1, Figure 4C), in addition to the endogenous HLA
269 alleles. Strikingly, we found that the three nonC-TL evaluated were frequently expressed and detected by
270 nonC-TL-specific T cells in patient-derived TCL, as observed by 4-1BB upregulation when the relevant HLA
271 was expressed (Figure 4D). Of note, 5'U-HOXC13 and 5'U-ZKSCAN1 were detected in melanoma, but also in
272 other less immunogenic tumor types such as gastrointestinal cancers (GI) or gynecological malignancies.
273 Furthermore, the recognition of several HLA-A*11:01⁺ TCL by nonC-TL-specific T cells without transfecting
274 any additional HLA, showed that nc-C5orf22 and 5'U-HOXC13 can be naturally processed and presented on
275 HLA-I (Figure 4D). Altogether, these results show that nonC-TL are shared across tumor types and can be
276 naturally presented and recognized by T cells.

277 **TCRs targeting nonC antigens can display cancer-specific recognition**

278 A potential concern that has not yet been addressed regarding the therapeutic targeting of nonC-TL
279 is whether they are tumor specific. To investigate this, we analyzed the RNA expression of the canonical
280 genes encoding for the three immunogenic nonC-TL in several solid tumors and matched healthy tissues
281 from repository data (GEPID). We compared their expression pattern to PMEL and MLANA as examples of
282 melanoma-associated antigens, and MAGEA3 and MAGEC2 representing CGA (Figure 5A). Whereas C5orf22
283 and 5'U-ZKSCAN canonical genes displayed a variable but ubiquitous expression among tissues, the
284 expression of HOXC13 canonical gene in healthy tissues appeared to be restricted to melanocytes,
285 resembling the expression pattern of MLANA. This raised the possibility that the identified immunogenic
286 nonC-TL might not be tumor specific. However, RNA transcript level cannot distinguish canonical from
287 aberrant translation. In addition, contrary to the RNA-seq data analysis, the healthy immunopeptidome
288 data that was used to select for nonC HLA-I ligands derived from ORFs absent in non-malignant cells
289 suggested that the nonC translation of these peptides was tumor specific.

290 To gain further insights into the selective expression of these nonC-TL in tumor cells and their
291 applicability as targets for cancer immunotherapy, we empirically evaluated the expression and translation
292 of the selected immunogenic nonC-TL in several human healthy cell types by exploiting the ability of
293 antigen-specific T cells to detect their cognate peptides with high sensitivity. To this end, we first
294 sequenced the TCR locus of the nonC-TL-specific T cells identified by IVS and the most frequent TCR- α/β
295 pairs of each of the populations were cloned into a retroviral vector and used to transduce PBL.
296 Additionally, given that the canonical HOXC13 gene expression pattern resembled MLANA, we generated
297 DMF5 TCR-transduced cells as an example of a TCR tested in clinical trials, which recognizes the melanoma-
298 associated antigen MART-1₂₇₋₃₅ (encoded by MLANA and restricted to HLA-A*0201) that is expressed both
299 in melanoma cells and healthy melanocytes (8). Given that the TCRs recognizing nonC-TL were CD8-
300 dependent, as opposed to the MART-1-specific TCR (Figure 5B), all PBL TCR transduced cells were sorted
301 based on CD8 and mTCR expression (CD8⁺mTCR⁺). Peptide titration experiments to measure functional
302 avidity of TCR transduced cells evidenced that nc-C5orf22 and 5'U-HOXC13-specific TCRs required higher
303 concentrations of minimal peptide to become activated, while 5'U-ZKSCAN1 and MART-1 TCR transduced
304 cells were more sensitive at detecting their cognate antigen (Figure 5C).

305 Next, the four antigen-specific CD8⁺ mTCR⁺ cells were co-cultured with human cells of different
306 origin, including normal melanocytes, cardiac myocytes, renal epithelial, and fibroblast, as well as a few of

307 the previously tested melanoma cell lines. As in the previous experiment used to evaluate the expression of
308 nonC-TL antigens in patient-derived TCL (Figure 4D), expression of the specific HLA alleles restricting
309 antigen recognition of the TCRs evaluated was exogenously enforced in the target cells and T-cell activation
310 was evaluated by measuring 4-1BB upregulation in mTCR⁺ cells by flow cytometry following co-culture
311 (Figure 5D and Supplemental Figure 14). As expected, MART-1 TCR transduced cells strongly recognized
312 human melanocytes electroporated with the HLA-A*02:01, as well as three out of the four patient-derived
313 melanoma cell lines tested. Surprisingly, cardiac myocytes were also recognized by MART-1 TCR transduced
314 cells, albeit to a limited extent. 5'U-ZKSCAN1 TCR transduced cells displayed preferential recognition of
315 melanoma cells compared to normal melanocytes and cardiac myocytes when target cells were
316 electroporated with the relevant allele HLA-A*68:01. Importantly, 5'U-HOXC13 displayed recognition of
317 two of the four melanoma cell lines included but did not recognize cardiac myocytes and barely recognized
318 normal melanocytes when electroporated with the corresponding allele HLA-A*11:01. The lower sensitivity
319 of the nonC C5orf22 TCR and/or limited expression of the antigen precluded us from reaching a conclusion
320 regarding the tumor specific expression of this antigen. Overall, these results indicate that the 5'U-HOXC13
321 peptide is the nonC antigen with the highest tumor specificity followed by 5'U-ZKSCAN1. Importantly, both
322 nonC antigens displayed a superior tumor specific profile compared to MART-1. Although we cannot rule
323 out the possibility that these antigens could be expressed and translated in additional normal cell types,
324 our findings suggest that the aberrant translation giving rise to the nonC peptides studied occurs
325 preferentially in tumor cells rather than in normal cells. Overall, our results demonstrate that nonC-TL are a
326 promising alternative source of tumor antigens to neoantigens, CGA and TAA not only because they can be
327 naturally presented but also because they can be immunogenic and expressed across diverse tumor types
328 but not, or at very low levels, in healthy cells.

329 **Discussion**

330 Tumor antigens play an integral role driving protective or therapeutic antitumor immunity. Recent
331 evidence suggests that peptides derived from nonC proteins can be systematically detected through
332 proteogenomics and are specifically presented on HLA-I by tumor cells. However, their contribution to
333 tumor immune surveillance and their immunogenicity has not been explored in detail.

334 The proteogenomics pipeline we used, Peptide-PRISM, is independent of RNA-seq and Ribo-seq but
335 enables the detection of HLA-I ligands potentially originating from any region of the genome, including CDS,
336 UTR, off-frame, ncRNA, intronic and intergenic regions (Figure 1A). Like previous immunopeptidomics
337 studies (20–24,31,33,34,39) , we observed that nonC HLA-I ligands were frequently detected across
338 different cancer types (Figure 1B). Because we were interested in tumor-specific candidates we used
339 healthy immunopeptidome data to exclude peptides derived from ORFs present in non-malignant cells. As
340 a result, 61.5% of the nonC HLA-I-ligands detected were preferentially presented by tumors, referred to as
341 nonC-TL (Figure 1C). Importantly, we studied the repertoire of presented tumor antigen candidates in 9
342 patient-derived TCL. Our work shows that nonC-TL (n=507) outnumber the HLA-I ligands derived from
343 conventional tumor antigens such as mutations (n=33), CGA antigens (n=36) and melanoma-associated
344 antigens (n=24) (Figure 2A). In line with previous reports (36–38), the number of HLA-I ligands derived from
345 NSM was relatively low compared to the NSM identified by WES (Figure 2C). Notably, our data adds a
346 considerable number of mutated HLA-I peptides to those identified through immunopeptidomics so far,
347 underscoring the performance of Peptide-PRISM at detecting neoantigen candidates.

348 NonC proteins were frequently presented in patient-derived TCLs, being the main source of
349 candidate tumor antigens, but pre-existing T-cell responses targeting nonC-TL were not detected in any of

350 the patients studied (Figure 3F and Supplemental Figure 15). In contrast, nearly 65% of the antigens
351 recognized by T cells were derived from mutations (n=13), 20% from CGA (n=4) and 15% from melanoma-
352 associated antigens (n=3) (Table 1 and Supplemental Figure 15). Moreover, the isolated antigen-specific T
353 cells recognized the autologous TCL (Supplemental Figure 7 and Figure 10), demonstrating that the
354 peptides identified were bona fide tumor antigens. To our knowledge, the existence and frequency of
355 naturally occurring T cells targeting nonC-TL compared to conventional tumor antigens has not previously
356 been investigated in such detail. The majority of studies identifying nonC peptides presented on HLA-I did
357 not investigate their immunogenicity in patients (20,22–24,31,33,40). A few explored their immunogenicity
358 through *in vitro* sensitization of PBL from healthy donors which detects naïve rather than antigen-
359 experienced T cells (21,41–43), or immunized mouse models (25). Only one proteogenomics report
360 evaluated T-cell responses against nonC HLA-I ligands as well as other relevant tumor antigens derived from
361 melanoma-associated antigens and CGA identified from patient-derived TCL and tumor samples(34).
362 Although they reported some degree of reactivity to one of the 571 nonC HLA-I peptides evaluated, our
363 results are in accordance with their findings since the percentage of reactive peptides clearly favored
364 melanocyte differentiation antigens, supporting that nonC HLA-I ligands are not as immunogenic.

365 One limitation of our study lies in the nature of the proteogenomics approach used combined with
366 the stringent and uniform 1% FDR threshold set to select the tumor antigen candidates. Although this
367 pipeline potentially detects peptides originating from any region of the genome, the FDR calculation using a
368 stratified mixture model could result in an underestimation of nonC ligands with an increased search space,
369 for example intergenic regions. Consequently, some of the previously described nonC sources were not
370 properly interrogated such as endogenous retroviral elements (ERE), or not considered in this study such as
371 RNA editing or peptide splicing (44,45). Overall, our findings predict a limited contribution of nonC-TL to
372 tumor immune surveillance.

373 Despite we could not detect recall T-cell responses to nonC-TL, we were able to isolate and expand T
374 cells specifically targeting three nonC-TL through IVS of non-autologous HLA-A*11:01⁺ PBL. We found that
375 two immunogenic nonC-TL derived from the aberrant translation of 5'UTR of HOXC13 and ZKSCAN1 genes
376 were frequently detected in patient-derived melanoma TCL as well as other less immunogenic tumor types
377 such as GI or Gyn. In addition, an immunogenic nonC-TL derived from a non-coding spliced variant of
378 C5orf22 gene was also detected in several melanoma TCL. These results revealed that nonC-TL can be
379 immunogenic and shared across tumor types, thus representing attractive targets for off-the-shelf vaccines
380 or T-cell therapies.

381 The paradoxical lack of recognition of nonC-TL in cancer patients in light of the fact that at least a
382 fraction of these were proven to be immunogenic could be explained through different mechanisms. For
383 instance, we screened *ex vivo* expanded lymphocytes which frequently present a skewed oligoclonal TCR
384 repertoire, which could lead to the depletion of some tumor-reactive clones (46). Although this could be
385 the case, theoretically, this would negatively impact on the T-cell recognition of all antigen categories
386 equally. Another possible explanation is that the level of expression of nonC-TL may be sufficient for
387 presentation on tumor HLA-I, but inadequate for efficient cross-presentation *in vivo*, leading to defective
388 priming of T cells. In line with this hypothesis, nonC peptides are thought to be less abundant and largely
389 originated from disordered or unstable proteins with shorter half-lives compared to functionally annotated
390 proteins (22,47). In addition, some nonC ORF are so small that they do not require processing (33). These
391 characteristics can facilitate the accessibility of nonC peptides into the HLA-I antigen presentation pathway
392 (47,48). Moreover, some studies have demonstrated that rapidly degraded proteins and minimal epitopes
393 are unable to provoke cross-priming by APC as opposed to stable, full-length antigens (49). Altogether, this

394 data suggests that the native characteristics of the aberrant translation events giving rise to nonC-TL (i.e.
395 low abundance and instability) could account, at least in part, for the lack of recognition in cancer patients.
396 An alternative explanation for our findings is that nonC-TL could also be presented by mTEC cells in the
397 thymus, leading to partial central tolerance and, consequently, limiting the abundance of T cells targeting
398 nonC-TL in periphery. This, combined with the low level of expression and/or poor priming could hamper
399 the detection of antigen-experienced T cells targeting nonC-TL in cancer patients.

400 In our work, we addressed the tumor specific expression of nonC antigens, an essential aspect for the
401 development of immunotherapeutic interventions. Previous studies have used healthy RNA-seq data to
402 exclude nonC HLA-I ligands presented in healthy tissues. Alternatively, Ribo-seq could potentially be used to
403 select tumor-specific nonC ORF. However, this technique is relatively new, the sensitivity is still limited and
404 little data from healthy tissue is currently available. Instead, we leveraged a healthy immunopeptidome
405 dataset to select nonC HLA-I ligands absent in non-malignant cells. Although immunopeptidomics is less
406 sensitive, we believe it is more relevant, since it can detect peptides derived from both canonical and
407 aberrant translation. To gain additional insights into the tumor specificity of the three immunogenic nonC
408 identified, we indirectly evaluated their expression and translation in healthy human cells derived from
409 several vital organs as well as melanocytes by using lymphocytes transduced with antigen specific TCRs. Our
410 results revealed that the 5'U-HOXC13 peptide was the nonC antigen with the highest tumor-specificity,
411 since TCR-transduced T cells targeting this antigen recognized several TCL, but barely melanocytes or any
412 other healthy human cell tested. In fact, both 5'U-HOXC13 and 5'U-ZKSCAN1 nonC antigens displayed a far
413 superior tumor specific profile compared to MART-1, as TCR DMF5 displayed strong recognition of
414 melanocytes (>90%). Unexpectedly, DMF5 TCR transduced T cells recognized cardiac myocytes at a similar
415 level as TCR transduced T cells targeting the nonC-TL 5'U-ZKSCAN1 (10-20%). Although DMF5 TCR has
416 shown objective tumor responses in patients it also evidenced severe on-target toxicities in skin, eyes, and
417 ears due to the high expression of MART-1 in melanocytes(8), but toxicities related to cardiac myocyte
418 recognition has never been reported. These findings suggest that the low level of expression of these nonC-
419 TL in healthy tissues that we observed (Figure 5D) are insufficient to trigger undesired off-tumor toxicities.
420 Overall, our data supports that nonC-TL can display a tumor-specific profile that is compatible with their
421 use as therapeutic targets. Nonetheless, these data must be interpreted with caution, since we cannot rule
422 out the possibility that these immunogenic nonC-TL are expressed and translated in other healthy cells.

423 Overall, our results demonstrate that nonC-TL constitute an abundant source of candidate tumor
424 antigens compared to peptides derived from mutations, CGA, or tissue differentiation antigens. NonC-TL
425 are shared across tumor types and can be naturally presented by cancer cells and recognized by T cells.
426 More importantly, they are not detected or at very low levels in healthy cells. Therapeutic interventions
427 such as vaccines or TCR gene engineered T cells targeting nonC-TL could overcome the defective
428 endogenous T cell responses observed in cancer patients by enhancing the *de novo* priming of T cells or
429 administering large numbers of effector cells that can directly attack tumor cells. In fact, it is tempting to
430 speculate that the lack or defective T-cell response to nonC tumor antigens in cancer patients could be
431 advantageous, since these antigens and the HLA presenting them are less exposed to immune selective
432 pressure and, consequently, tumors would less likely present antigen escape variants selected through
433 immunoediting. Our findings predict a limited contribution of nonC-TL to cancer immunosurveillance and,
434 at the same time, underscore nonC-TL as a promising source of antigens for the development for
435 therapeutic interventions.

436 **Methods**

437 **Patient characteristics**

438 Patients Gyn-1, Gyn-2, Gyn-3, Gyn-4, H&N-1, H&N-3, Mel-1, Mel-2 and Mel-3 were chosen for this study
439 on the basis of availability of autologous tumor cell line and matched lymphocytes. Patient characteristics
440 are summarized in Supplemental Table 1.

441 **Establishment of patient-derived TCL**

442 A small fragment (2-4 mm³) of tumor biopsies or surgically resected tumor was cultured in RPMI 1640 plus
443 (Lonza) containing 10% FBS Hyclone (GE Healthcare), 100 U/mL penicillin (Lonza), 100 µg/mL streptomycin
444 (Lonza) and 25 mM HEPES (Thermo Fisher Scientific) at 37°C in 5% CO₂. The medium was replaced once
445 every month until the TCL was established and then further expanded in T2 media containing RPMI 1640
446 plus (Lonza), 10%-20% FBS (Gibco), depending on the TCL, 100 U/mL penicillin (Lonza), 100 µg/mL
447 streptomycin (Lonza) and 25 mM HEPES (Thermo Fisher Scientific) or cryopreserved until used. TCL were
448 regularly tested for mycoplasma and were authenticated based on the identification of patient-specific
449 somatic mutations and HLA molecules.

450 **TIL expansion**

451 Small tumor fragments (2-4 mm³) were cultured in individual wells of a 24-well plate in T-cell media
452 consisting of RPMI 1640 plus (Lonza) supplemented with 10% human AB serum (BST), 100 U/mL penicillin
453 (Lonza), 100 µg/mL streptomycin (Lonza), 2 mM L-Glutamine (Lonza), 25 mM HEPES (Thermo Fisher
454 Scientific) and 6e6 IU IL-2 (Proleukin) at 37°C and 5% CO₂. Fresh media containing IL-2 was added on day 5
455 and media was changed, or TIL were split when confluent every other day thereafter. T cells were
456 expanded independently for 15-30 days and cryopreserved until use. In some cases, T cells underwent a
457 rapid expansion protocol (REP), as explained below.

458 **Rapid expansion protocol (REP)**

459 T cells were expanded for 14 days using 30 ng/mL anti-CD3 (OKT3, Biolegend), 3e3 IU/mL of interleukin IL-2
460 (Proleukin) and irradiated allogeneic PBMC (50 Gy) pooled from three donors as feeder cells in T-cell
461 medium RPMI 1640 plus (Lonza):AIM-V (Gibco) containing 5% human AB serum (BST), 100 U/mL penicillin
462 (Lonza), 100 µg/mL streptomycin (Lonza), 2mM L-Glutamine (Lonza), 12.5 mM HEPES (Thermo Fisher
463 Scientific). After day 6, half of the medium was replaced with fresh T-cell medium containing IL-2 every
464 other day. Cells were split when confluent, harvested on day 14, and cryopreserved until use.

465 **PBMC isolation**

466 Peripheral blood mononuclear cells (PBMC) were obtained using a Ficol density gradient (Lymphoprep,
467 Stem cell) from pheresis or whole blood and cryopreserved for cell sorting, DNA extraction for WES and to
468 expand B cells *ex vivo*.

469 **T cell sorting from PBL**

470 PBLs were sorted based on the expression of surface markers previously described to enrich for tumor-
471 reactive T cells in peripheral blood such as PD-1 (50). Briefly, PBMCs were thawed and rested overnight
472 without cytokines. Following CD8⁺ enrichment using CD8 microbeads (Miltenyi Biotec), the Fc receptor was
473 blocked (Miltenyi Biotec) and cells were stained with the following antibodies for 30 minutes at 4°C: CD3-
474 PECy7 (BD, clone SK7, 0.5:50), CD8-APCH7 (BD, clone SK1, 1:50), PD1-PE (Biolegend, clone EH12.2H7,
475 0.75:50), CD38-APC (Biolegend, clone HIT2, 0.5:50) and HLA-DR BV605 (Biolegend, clone L243, 0.75:50).

476 CD3⁺CD8⁺ cells expressing PD1hi alone or in combination with HLA-DR and CD38 were sorted in BD FACS
477 AriaTM and expanded using a REP as previously specified.

478 **Generation of autologous APC**

479 B cells were isolated from cryopreserved PBMCs by positive selection using CD19⁺ microbeads (Miltenyi
480 Biotec) and expanded through CD40-CD40L stimulation by culturing cells for 4-5 days with irradiated
481 NIH3T3 feeder cells constitutively expressing CD40L at 37°C in 5% CO₂ in B cell medium. Iscove's IMDM
482 media (Gibco) containing 10% human AB serum (Biowest), 100U/mL Penicillin and 100 µg/mL streptomycin
483 (Lonza), 2 mM L-Glutamine (Lonza), and supplemented with 200 U/ml IL-4 (Peprotech). Up to three rounds
484 of stimulation and expansion were performed consecutively. B cells were cryopreserved from day 5 to 6
485 until use. When used after cryopreservation, B cells were thawed in B cell medium containing DNase
486 (Pulmozyme, Roche) 20 h before use in co-culture assays. Alternatively, CD4⁺ T cells were isolated from
487 PBMCs by positive selection using CD4⁺ microbeads (Miltenyi Biotec) or FACS sorting and subsequently
488 expanded through a REP.

489 **Peptides**

490 The amino acid sequences of the identified tumor antigen HLA-I ligands were purchased from JPT Peptide
491 Technologies (Berlin, Germany) as crude and used for screening, IVS, and MS validation with synthetic
492 peptides. HPLC peptides were supplied by JPT Peptide Technologies (Berlin, Germany) and used in co-
493 culture experiments to confirm the reactivities. Selected endogenous HLA-I ligands were ordered from
494 Thermo Fisher Scientific as crude (PePotec grade 3) with one stable isotope-labeled amino acid and used
495 for PRM validation (See Supplemental data 3).

496 **Cloning, *in vitro* transcription of RNA, and electroporation**

497 The HLA sequences of interest or predicted ORF of the immunogenic nonC-TL peptides were cloned into
498 pcDNA3.1 using BamH1 and EcoR1 containing a Kozak motif upstream of the start codon. HLA-I sequences
499 were obtained from IPD-IMGT/HLA and codon-optimized. The predicted ORF were constructed from the
500 second nearest upstream in-frame start codon (ATG, CTG, or GTG) to the first in-frame stop codon
501 downstream; the sequence was not codon optimized nor additional start codons were added. All the
502 plasmids were synthesized by Genscript.

503 For *in vitro* transcription (IVT) of RNA the plasmids were linearized with Not-I followed by phenol-
504 chloroform extraction and precipitation with sodium acetate and ethanol. Next, 1 µg of DNA was used as a
505 template to generate RNA by IVT using HiScribe# T7 ARCA mRNA Kit with tailing (New England) following
506 manufacturer's instructions. RNA was precipitated using LiCl₂, resuspended at 1 µg/µL in molecular grade
507 H₂O, and stored at -80° until use.

508 From 0.5-1e6 TCL, healthy human cells, and B cells were harvested and resuspended in 100 µl of Opti-MEM
509 media (Gibco) and transferred into a sterile 0.2 cm cuvette (VWR electroporation cuvettes). From 4 to 8 µg
510 of RNA encoding for the sequence of interest were added for electroporation. Cells were electroporated at
511 150 V, 20 ms, and 1 pulse using an ECM 830 BTX-Electroporator. After electroporation, cells were
512 resuspended in pre-warmed specific media containing DNase (Pulmozyme, Roche). After 20 h cells at 37°C
513 and 5% CO₂, cells were harvested, washed with PBS, and used in co-culture assays. A GFP RNA
514 electroporation control was included for each cell line and assessed by Flow cytometry as a transfection
515 control.

516 **Co-culture assays: IFN- γ enzyme-linked immunospot (ELISPOT) assays and detection of**
517 **activation marker 4-1BB using flow cytometry.**

518 T cells were thawed into T-cell medium supplemented with 3,000 IU IL-2 (Proleukin) and DNase
519 (Pulmozyme, Roche) three to four days before coincubation with target cells. All co-cultures were
520 performed in the absence of exogenously added cytokines. Cells were stained with CD3-APCH7 (BD, clone
521 SK7, 0.3:40), CD8-PECy7 (BD, clone RPA-T8, 0.1:40), CD4-PE (BD, RPA-T4, 0.3:40) and CD137-APC (BD, clone
522 4B4-1, 0.5:40), and in some cases mTRB-FITC (eBiosciences, clone H57-597, 0.2:40) for 30 minutes at 4°C,
523 washed with staining buffer containing PI (1:2000) and acquired in BD FACSLyric™, BD FACSCanto™ or BD
524 FACSLyric™. In parallel, IFN- γ secretion was detected using IFN- γ capture and detection antibodies
525 (MABtech technologies) assessed by ELISPOT assay following manufacturer instructions. ELISPOT plates
526 were analyzed and counted in ELISPOT reader. For all the assays, plate-bound OKT3 (1 μ g/mL; Biolegend)
527 was used as a positive control. Media, and/or autologous APC pulsed with irrelevant peptides were used as
528 negative controls.

529 For the detection of recall T-cell responses, from 2e4 to 5e4 *ex vivo* expanded TIL, sorted PBL or
530 enriched populations of tumor-reactive lymphocytes were co-cultured with 1e5 to 2e5 peptide-pulsed
531 autologous APC (either B cells, or CD4⁺ T cells). T-cell reactivities were considered positive if the number of
532 IFN- γ spots were greater than double the amount of the irrelevant control condition and greater than 40
533 spots. Additionally, reactivities had to be observed in at least two independent experiments. Crude
534 peptide preparations were used for screening, and the reactivities were further confirmed with HPLC
535 grade peptides. Experiments were performed at least twice.

536 **Enrichment of tumor-reactive and antigen-specific T cells**

537 Either expanded TIL, sorted PBL or IVS T cells were co-cultured with tumor cells or peptide-pulsed
538 autologous APC for 20 h. CD3⁺CD8⁺ cells expressing 4-1BB were sorted in BD FACS Aria™ or BD Influx™ and
539 expanded using a REP as previously specified. The same antibodies and dilutions used for co-cultures
540 described above were scaled up for staining 4-1BB⁺ T cells.

541 **HLA restriction element determination**

542 COS-7 cells were transfected with plasmids encoding the individual HLA molecules using Lipofectamine
543 2000 (Life Technologies). After resting overnight, cells were harvested and pulsed with the corresponding
544 peptides for 2 h, washed, and used as targets in co-culture assays.

545 ***In vitro* sensitization of PBL**

546 HLA-A*11:01 donor PBMCs were stimulated with 5 independent peptide pools (PP) each containing up to
547 35 nonC-TL selected by the prediction score to bind to HLA-A*11:01 according to NetMHCpan4.0. Cells
548 underwent three consecutive rounds of stimulation every 7 days with 0.25 μ g/mL per peptide and a
549 combination of IL-21, IL-7 and IL-2. More specifically, at day 0, 5e6 donor PBMC were cultured in 24-well
550 plates with OpTmizer™ media (Gibco) containing IL-21 (Peprotech 25 ng/mL) and the corresponding PP at
551 0.25 μ g/ml per peptide. On day 6, IL-2 (Proleukin 18 IU/mL) and IL-7 (Peprotech 10 ng/mL) were added. For
552 STIM2 (day 7) and STIM3 (day 14), T cells from the previous STIM were harvested, counted, and re-
553 stimulated with autologous irradiated PBMC (50 Gy) pulsed with the corresponding PP at 1:10 ratio.
554 Thereafter, fresh OpTmizer™ media (Gibco) containing IL-2 (18 IU/mL) and IL-7 (10 ng/mL) was replaced
555 when medium looked acidified, or cells required splitting.

556 *De novo* T-cell responses were evaluated after three stims by co-culturing IVS T cells with autologous B cells
557 pulsed with the corresponding PP and analyzing 4-1BB upregulation by flow cytometry as described above.

558 T cells recognizing the corresponding PP were sorted based on 4-1BB expression and expanded for 14 days
559 in a REP (Enrichment of antigen-specific T cells). To identify the specific peptide recognized within the PP,
560 sorted populations were co-cultured with B cells pulsed with individual peptides. The recognition was
561 confirmed using HPLC purified peptides.

562 **TCR sequencing and PBL transduction**

563 The TCR locus was sequenced by multiplex single-cell RNA sequencing of enriched antigen-specific T-cell
564 populations. The samples were multiplexed using TotalSeq™ barcodes. Sequencing was done on an Illumina
565 NS6000 with an S1 flowcell and v1 chemistry. Mapping, quantification, and clonotype definitions were done
566 using cell ranger multi software (version 6.1.1 using the reference vdj_GRCh38_alts_ensembl-5.0.0).
567 Demultiplexing and subsequent analysis was using the packages Seurat (version 4.0.3) and scRepertoire
568 (version 1.3.5); Seurat::HTODemux was run using default parameters to obtain singlets.

569 TRA V-J-encoding sequences and TRB V-D-J-encoding sequences were combined to sequences encoding the
570 mouse constant TRA and TRB chains (51), respectively. Mouse constant regions were modified, as
571 previously described (52,53) . The full-length TRB and TRA chains were cloned separated by a furin SGSG
572 P2A linker into pMSGV1 retroviral vector (GenScript). Transient retroviral supernatants were generated by
573 transfecting the vector encoding the TCR of interest (MSGV1) and envelope (RD114) into 293GP cells using
574 Lipofectamine 2000 (Life Technologies). PBLs were activated in T cell medium supplemented with 50 ng/mL
575 anti-CD3 and 300 IU/mL IL-2 for 3 days before retroviral transduction. Retroviral supernatants were
576 harvested at 24 and 48 hours, centrifuged to discard cell debris, and diluted 1:1 with medium and used to
577 transduce the activated lymphocytes using the spinoculation method, as previously described.(15)

578 **Normal human cell lines**

579 Normal human cell lines were purchased from Promocell, thawed and cultured following manufacturer's
580 instructions in the recommended media without antibiotics. Cells were split when confluent with
581 Dettaching kit (Promocell), cultured at the recommended concentration and expanded no more than 4
582 passages until use. HCM-c (Cat: C-128810) were cultured in myocyte growth medium (Cat n°: C-39275).
583 HREpC-c (CatC-12665) were cultured in Renal Epithelial Cell GM media (Cat n°: C-39606). HSAEpC-c (Cat: C-
584 12642) were cultured in Small Airway Epithelial cell GM (Cat n°: C-39175). NHEM.f-c (Cat: C-12400) were
585 cultured in Melanocyte growth medium (Cat n°: C-39415).

586 **Whole exome sequencing**

587 To identify the tumor-specific NSM, genomic DNA was purified from a cell pellet of patient-derived TCL and
588 matched PBMC. WES libraries were generated by exome capture of approximately 20,000 coding genes
589 using SureSelect human All exon V6 kit (Agilent Technologies) and paired-end sequencing was performed
590 on a HiSeq sequencer (Illumina) at Macrogen. The average sequencing depth ranged from 100-150 for each
591 of the individual libraries generated. Alignments of WES to the reference human genome build hg19 were
592 performed using novoalign MPI from novocraft. Duplicates were marked using Picard's MarkDuplicates
593 tool. Insertion and deletion (indel) realignment and base recalibration were performed according to GATK
594 best-practices. Samtools was used to create tumor and normal pileup files. Four independent mutation
595 callers (Varscan, SomaticSniper, Mutect and Strelka) were used to call somatic NSM. The genomic
596 coordinates from VCF files containing tumor-specific mutations were converted from hg19 to hg38
597 assemblies.

598 **GTEX and TCGA RNA analyses**

599 TCGA and GTEX data from paired tumor and healthy data was obtained and analyzed using GEPIA
600 (02/05/2022) and plotted using R. RNA levels are expressed as Log₂ (TPM+1), the density of color in each
601 block represents the median expression value of a gene in a given tissue, normalized by the maximum
602 median expression value across all blocks. Abbreviation of tumor types: ACC;Adrenocortical carcinoma,
603 BLCA;Bladder Urothelial Carcinoma, BRCA;Breast invasive carcinoma, CESC;Cervical squamous cell
604 carcinoma and endocervical adenocarcinoma, CHOL;Cholangio carcinoma, COAD;Colon adenocarcinoma,
605 DLBC;Lymphoid Neoplasm Diffuse Large B-cell Lymphoma, ESCA;Esophageal carcinoma, GBM;Glioblastoma
606 multiforme, HNSC;Head and Neck squamous cell carcinoma, KICH;Kidney Chromophobe, KIRC;Kidney renal
607 clear cell carcinoma, KIRP;Kidney renal papillary cell carcinoma, LAML;Acute Myeloid Leukemia, LGG;Brain
608 Lower Grade Glioma, LIHC;Liver hepatocellular carcinoma, LUAD;Lung adenocarcinoma, LUSC;Lung
609 squamous cell carcinoma, MESO;Mesothelioma, OV;Ovarian serous cystadenocarcinoma, PAAD;Pancreatic
610 adenocarcinoma, PCPG;Pheochromocytoma and Paraganglioma, PRAD;Prostate adenocarcinoma,
611 READ;Rectum adenocarcinoma, SARC;Sarcoma, SKCM;Skin Cutaneous Melanoma, STAD;Stomach
612 adenocarcinoma, TGCT;Testicular Germ Cell Tumors, THCA;Thyroid carcinoma, THYM;Thymoma,
613 UCEC;Uterine Corpus Endometrial Carcinoma, UCS;Uterine Carcinosarcoma,UVM;Uveal Melanoma.

614 **Purification of HLA-I peptides**

615 Purified anti-HLA-I clone W6/32 (ATCC® HB95) antibodies were cross-linked to protein-A Sepharose 4B
616 conjugate beads (Invitrogen) with dimethyl pimelimidate dihydrochloride (Sigma-Aldrich) in 0.2 M Sodium
617 Borate buffer pH 9 (Applichem). From 5e7 to 3e8 tumor cells (See Supplemental Table 1) were snap-frozen,
618 thawed, and lysed with PBS containing 0.6% CHAPS (Applichem) and Protease inhibitor Cocktail Complete
619 (Roche). The cell lysates were sonicated (Misonix 3000) and cleared by centrifugation for 1 h at max speed
620 to obtain the soluble fraction containing the pHLA complexes. The HLA-I affinity chromatography was
621 performed using a 96-well single-use micro-plate with 3 µm glass fiber and 10 µm polypropylene
622 membranes (Agilent). Sep-Pak tC18 100 mg Sorbent 96-well plates (Waters) were used for peptide
623 purification and concentration as previously described (54). Peptides were eluted with 500 µl of 32,5% ACN
624 in 0.1% TFA, lyophilized, and further cleaned and desalted with TopTips (PolyLC Inc.)

625 **LC-MS/MS acquisition**

626 Acclaim Pep-Map nanoViper, C18 (Thermo Scientific) at a flow rate of 15 µl/min using a Thermo Scientific
627 Dionex Ultimate 3000 chromatographic system (Thermo Scientific). Peptides were separated using a C18
628 analytical column of 75 µm × 250 mm, 1.8 µm, 100Å (Waters) or 25 µm × 250 mm, 1.8 µm, 100Å (Waters).
629 Orbitrap Fusion Lumos™ Tribrid (Thermo Scientific) mass spectrometer was operated in data-dependent
630 acquisition (DDA) mode. Survey MS scans were acquired in the orbitrap with the resolution (defined at 200
631 m/z) set to 120,000. The top speed (most intense) ions per scan were fragmented in the linear ion trap
632 (CID) and detected in the Orbitrap with the resolution set to 30,000. Quadrupole isolation was employed to
633 selectively isolate peptides of 400-600 m/z. Included charged states were 2 and 3. Target ions already
634 selected for MS/MS were dynamically excluded for 10 s.

635 **Mass spectrometry data analysis of HLA-I peptides with Peptide-PRISM**

636 Peptide-PRISM was used as previously described (20) without including random substitutions nor
637 proteasome-spliced peptides. Briefly, for each identified fragment ion mass spectrum the Top 10
638 candidates were first identified by *de novo* sequencing with PEAKS X and later aligned to a database
639 containing a 3-frame translated transcriptome (Ensembl90) and 6-frame translated genome (hg38).
640 Additionally, vcf files from somatic mutation calling were used to interrogate NSM in a personalized

641 fashion. All identified string matches were categorized into CDS (in-frame with annotated protein), 5'-UTR
642 (contained in annotated mRNA, overlapping with 5'-UTR), Off-frame (off-frame contained in the coding
643 sequence), 3'-UTR (all others that are contained in an mRNA), ncRNA (contained in annotated ncRNA),
644 Intronic (intersecting any annotated intron) or Intergenic. Then, for each fragment ion mass spectrum, the
645 category with the highest priority (CDS>5'-UTR>Off-frame>3'-UTR>ncRNA>Intronic>Intergenic) was
646 identified, and all other hits among the 10 *de novo* candidates were discarded. The FDR was calculated for
647 each category in a stratified mixture model considering the peptide length and database size. The same
648 pipeline was applied to immunopeptidomics data obtained from HLA ligand atlas (55) including various
649 tissues and HLA alleles. The predicted ORF from the nonC HLA-I ligands identified in the healthy
650 immunopeptidome were retrieved and used to filter out the nonC HLA-I ligands from our tumor samples
651 derived from the same ORF. All identified peptides were filtered to FDR 0.01. In addition, peptides with a *de*
652 *novo* score (ALC) smaller than 30 and the sequences that could not be unequivocally assigned to a single
653 category (Top location count=1) were filtered out (Supplemental Data 2). For peptides derived from NSM,
654 the FDR was set at 0.02 (Supplemental Data 3).

655 **HLA-I typing and prediction of binding to patient-specific HLA molecules**

656 HLA typing was determined from the WES data using the PHLAT algorithm (Supplemental Data 1). Eluted
657 ligand likelihood (ELL) percentile rank scores for binding to the patient's HLA molecules were obtained for
658 all unique peptides ≥ 8 Aa eluted from TCL using NetMHCpan 4.0. The threshold for binding was set to <2%
659 tile rank.

660 **Validation of HLA-I peptides with synthetic peptides**

661 Spectrum validation of the experimentally eluted HLA-I ligand tumor antigen candidates was performed by
662 computing the similarity of the spectra acquired in the sample with the corresponding non-labeled
663 synthetic peptide from the library. Briefly, synthetic crude peptides obtained from JPT were acquired in a
664 pool using LC-MS/MS in conditions similar to those previously used to analyze samples to generate a
665 spectral library. Peptide sequences were identified by database search with PEAKS-X Pro using a database
666 containing Swiss-Prot as well as all the tumor antigen candidates interrogated. The search was exported as
667 "for third party" format and imported into Skyline software to generate the library. The experimentally
668 acquired HLA-I tumor samples were uploaded into Skyline and the similarity of the fragments (b/y ions)
669 from the library (synthetic) vs. endogenous (sample) were analyzed considering library dot product (dotp)
670 values, which range from 0 to 1 and, being dotp=1 the closest match. (See Supplemental Data 3).

671 **Validation of HLA-I peptides with isotope-labeled peptides**

672 For each selected peptide, a synthetic isotope-labeled peptide at one chosen amino acid was spiked into
673 the samples and used as an internal standard for Parallel Reaction Monitoring (PRM) detection. The
674 amount of internal standard peptide to be spiked in each sample was evaluated using dilution curves and
675 the final concentration was chosen based on a good chromatographic signal and no trace detectable of
676 potential unlabeled traces from the synthetic internal standard. For Mel-3 TCL 30% of the sample (total of
677 5×10^7 cells) and for Mel-1 50% of the sample (total 1×10^8) was analyzed by PRM using different MS machines.
678 Orbitrap Eclipse (Thermo Fisher Scientific) coupled to an EASY-nanoLC 1000 UPLC system (Thermo Fisher
679 Scientific) with a 50 cm C18 chromatographic column. A PRM method was used for data acquisition with a
680 quadrupole isolation window set to 1.4 m/z and MS2 scans over a mass range of m/z 250-1800, with
681 detection in the Orbitrap mass analyzer at a 240 K resolution. MS2 fragmentation was performed using
682 HCD fragmentation at a normalized collision energy of 30%, the AGC was set at 100,000, and the maximum
683 injection time at 502 ms. All data were acquired with XCalibur software.

684 For data analysis fragment ion chromatographic traces corresponding to the targeted precursor peptides
685 were evaluated with Skyline software v.21.2. Verification of the endogenous peptides was based on: i) the
686 number of detected traces, ii) co-elution of endogenous traces, iii) co-elution of endogenous and internal
687 standard peptides, iv) correlation of the fragment ions relative intensities between endogenous and
688 internal standard peptides and, v) expected retention time.

689 **CRISPR/Cas9 Knock out**

690 Single guides RNA (sgRNA) targeting the predicted ORF for 5'U-HOXC13 were designed with CRISPOR tool
691 (<http://crispor.tefor.net/>). sgRNA specifically binding the genomic peptide location or upstream with the
692 highest predicted KO efficiency were selected. Next, sgRNA were cloned into lenti-Cas9-v2 (Addgene,
693 #52961) with BsmBI.

694 Lentiviral supernatants were generated by co-transfecting HEK293 cells with lenti-Cas9-v2 encoding the
695 sgRNA of interest, psPAX2 and pMD2G plasmids with PEI (Sigma) and non-supplemented DMEM media
696 (Gibco). Media was replaced after 12h with Opti-MEM (Gibco) containing 2% FBS (Gibco). Supernatants
697 were collected at 42-48 h after transfection and filtered through a 0.45 um low-protein binding filter
698 (Millipore). Patient-derived TCL were infected with lentiviral supernatants containing polybrene (Sigma)
699 final concentration of 8 ug/mL followed by spinoculation 900 g, 32°C, 50 min. Five days post-infection, T2
700 media (RPMI containing 10% FBS supplemented with Pen/Strep and L-Glut) was replaced with T2 media
701 containing puromycin 1 µg/mL to select the cells efficiently transduced. Thereafter, media was replaced
702 with fresh media containing puromycin when acidified or cells split when confluent. To evaluate the KO
703 efficiency, puromycin-resistant cells were used as targets in co-culture assays with 5'U-HOXC13 specific T
704 cells.

705 **Statistics**

706 Experiments were performed without duplicates, unless otherwise specified, data were reported as mean
707 +/- SEM. All experiments were repeated at least twice. For HLA-I ligand identification with Peptide-PRISM,
708 the FDR was calculated for each category in a stratified mixture model as previously described
709 (20) considering the peptide length and database size.

710 **Study approval**

711 Samples were obtained through a study approved by the Vall d'Hebron Hospital ethical committee
712 (PR(AG)482/2017). All patients provided a written, informed consent.

713 **Data Availability**

714 The mass spectrometry proteomics data have been deposited to the ProteomeXchange Consortium via the
715 PRIDE [1] partner repository with the dataset identifier PXD036856. The source data underlying Figure 5A
716 was downloaded from GEPIA (02/05/2022), data for Supplemental Figure 5 was downloaded from PRIDE
717 (identifiers PXD022150 and PXD004894). All other data are available from the corresponding author on
718 reasonable request.

719 **Author contribution**

720 A.G. conceived and designed the project and interpreted the results and wrote the manuscript.
721 M.L.R. designed, performed the experiments, and interpreted the analyses and wrote the manuscript.
722 F.E. and A.S. conceptualized and implemented the software for MS/MS data processing and FDR
723 calculations using Peptide-PRISM.
724 M.L.R. and A.Y.E. conducted the immunopeptidomics MS experiments.

725 M.L.R. generated patient reagents including TCL, TIL and sorted PBL.
726 M.L.R., A.G.G. and J.P. conducted the TIL experiments.
727 F.C. assisted in MS experimental design, data analyses and visualization.
728 J.J.G. performed the NGS analyses.
729 M.G. provided support with MS immunopeptidomics
730 JM.L., M.O.O, I.M., A.V., JM.P., X.M.G, I.B., E.M., E.G., provided valuable patient reagents used in this study.
731

732 **Acknowledgements**

733 We thank the patients for their participation in this study, Steven A. Rosenberg for providing valuable
734 reagents and support for NGS studies, R. Pujol for helpful scientific discussion, J.Gonzalez for bioinformatics
735 support, CRG/UPF Flow Cytometry Unit for assistance with cell sorting, and CRG/UPF and IRB Proteomics
736 Units for technical support. A.G. and this work were funded by the Comprehensive Program of Cancer
737 Immunotherapy & Immunology II (CAIMI-II) supported by the BBVA Foundation (53/2021), Institute Carlos
738 III (MS15/00058 and PI17/01085), AECC (IDEAS197PORT), and La Fundació La Marató de TV3 (201919-30).
739 We thank CERCA Programme / Generalitat de Catalunya for institutional support. M.L.R. was supported by
740 the Agència de Gestió d'Ajuts Universitaris i de Recerca (AGAUR) (2018FI_B 00946). A.G.G was supported
741 by Generalitat PERIS award (SLT017/20/000131). A.Y.E. was supported by the Agència de Gestió d'Ajuts
742 Universitaris i de Recerca (AGAUR) (2021 FI_B 00365). J.P. was supported by the Beatriu de Pinós
743 programme (BP 2018), cofounded by the Agency for Management of University and Research Grants
744 (AGAUR) and European Union's Horizon 2020.

745 **References**

- 746 1. Coulie PG, van den Eynde BJ, van der Bruggen P, Boon T. Tumour antigens recognized by T
747 lymphocytes: At the core of cancer immunotherapy. Vol. 14, Nature Reviews Cancer. 2014. p.
748 135–46.
- 749 2. Brichard V, Pel A van, W6lfel T, W61fel C, de Plaen E, Leth6 B, et al. The Tyrosinase Gene
750 Codes for an Antigen Recognized by Autologous Cytolytic T Lymphocytes on HLA-A2
751 Melanomas [Internet]. 1993. Available from: [http://rupress.org/jem/article-](http://rupress.org/jem/article-pdf/178/2/489/1267835/489.pdf)
752 [pdf/178/2/489/1267835/489.pdf](http://rupress.org/jem/article-pdf/178/2/489/1267835/489.pdf)
- 753 3. van der Bruggen P, Traversari C, Chomez P, Lurquin C, de Plaen E, van den Eynde B, et al. A
754 Gene Encoding an Antigen Recognized by Cytolytic T Lymphocytes on a Human. Vol. 254,
755 New Series. 1991.
- 756 4. Robbins PF, Morgan RA, Feldman SA, Yang JC, Sherry RM, Dudley ME, et al. Tumor regression
757 in patients with metastatic synovial cell sarcoma and melanoma using genetically engineered
758 lymphocytes reactive with NY-ESO-1. Journal of Clinical Oncology. 2011 Mar 1;29(7):917–24.
- 759 5. Morgan RA, Dudley ME, Wunderlich JR, Hughes MS, Yang JC, Sherry RM, et al. Cancer
760 Regression in Patients After Transfer of Genetically Engineered Lymphocytes. Science (1979)
761 [Internet]. 2006;314(5796):126–9. Available from:
762 www.sciencemag.org/cgi/content/full/1129003/DC1
- 763 6. Morgan RA, Chinnasamy N, Abate-Daga D, Gros A, Robbins PF, Zheng Z, et al. Cancer
764 Regression and Neurological Toxicity Following Anti-MAGE-A3 TCR Gene Therapy [Internet].
765 2013. Available from: <http://www.clinicaltrials.gov>
- 766 7. Linette GP, Stadtmauer EA, Maus M v, Rapoport AP, Levine BL, Emery L, et al. Cardiovascular
767 toxicity and titin cross-reactivity of affinity-enhanced T cells in myeloma and melanoma.
768 2013; Available from: www.bloodjournal.org

- 769 8. Johnson LA, Morgan RA, Dudley ME, Cassard L, Yang JC, Hughes MS, et al. Gene therapy with
770 human and mouse T-cell receptors mediates cancer regression and targets normal tissues
771 expressing cognate antigen. *Blood*. 2009;114(3):535–46.
- 772 9. Kristensen NP, Heeke C, Tvingsholm SA, Borch A, Draghi A, Crowther MD, et al. Neoantigen-
773 reactive CD8+ T cells affect clinical outcome of adoptive cell therapy with tumor-infiltrating
774 lymphocytes in melanoma. *Journal of Clinical Investigation*. 2022 Jan 18;132(2).
- 775 10. Parkhurst MR, Robbins PF, Tran E, Prickett TD, Gartner JJ, Li J, et al. Unique neoantigens arise
776 from somatic mutations in patients with gastrointestinal cancers. *Cancer Discov*. 2019 Aug
777 1;9(8):1022–35.
- 778 11. Stevanović S, Pasetto A, Helman SR, Gartner JJ, Prickett TD, Howie B, et al. Landscape of
779 immunogenic tumor antigens in successful immunotherapy of virally induced epithelial
780 cancer. *Science (1979)*. 2017 Apr 14;356(6334):200–5.
- 781 12. Hanada KI, Zhao C, Gil-Hoyos R, Gartner JJ, Chow-Parmer C, Lowery FJ, et al. A phenotypic
782 signature that identifies neoantigen-reactive T cells in fresh human lung cancers. *Cancer Cell*
783 [Internet]. 2022 Apr 13; Available from: <http://www.ncbi.nlm.nih.gov/pubmed/35452604>
- 784 13. Zacharakis N, Lutfi ;, Huq M, Seitter SJ, Kim SP, Gartner JJ, et al. Breast Cancers Are
785 Immunogenic: Immunologic Analyses and a Phase II Pilot Clinical Trial Using Mutation-
786 Reactive Autologous Lymphocytes. *J Clin Oncol* [Internet]. 2022;40:1741–54. Available from:
787 <https://doi>.
- 788 14. Samstein RM, Lee CH, Shoushtari AN, Hellmann MD, Shen R, Janjigian YY, et al. Tumor
789 mutational load predicts survival after immunotherapy across multiple cancer types. Vol. 51,
790 *Nature Genetics*. Nature Publishing Group; 2019. p. 202–6.
- 791 15. Tran E, Turcotte S, Gros A, Robbins PF, Lu YC, Dudley ME, et al. Cancer immunotherapy based
792 on mutation-specific CD4+ T cells in a patient with epithelial cancer. *Science (1979)*.
793 2014;344(6184):641–5.
- 794 16. Tran E, Robbins PF, Lu YC, Prickett TD, Gartner JJ, Jia L, et al. T-Cell Transfer Therapy Targeting
795 Mutant KRAS in Cancer. *New England Journal of Medicine*. 2016 Dec 8;375(23):2255–62.
- 796 17. Zacharakis N, Chinnasamy H, Black M, Xu H, Lu YC, Zheng Z, et al. Immune recognition of
797 somatic mutations leading to complete durable regression in metastatic breast cancer. *Nat*
798 *Med*. 2018 Jun 1;24(6):724–30.
- 799 18. Leidner R, Sanjuan Silva N, Huang H, Sprott D, Zheng C, Shih YP, et al. Neoantigen T-Cell
800 Receptor Gene Therapy in Pancreatic Cancer. *N Engl J Med* [Internet]. 2022 Jun
801 2;386(22):2112–9. Available from: <http://www.ncbi.nlm.nih.gov/pubmed/35648703>
- 802 19. Djebali S, Davis CA, Merkel A, Dobin A, Lassmann T, Mortazavi A, et al. Landscape of
803 transcription in human cells. *Nature*. 2012 Sep 6;489(7414):101–8.
- 804 20. Erhard F, Dölken L, Schilling B, Schlosser A. Identification of the cryptic HLA-I
805 immunopeptidome. *Cancer Immunol Res*. 2020 Aug 1;8(8):1018–26.

- 806 21. Laumont CM, Daouda T, Laverdure JP, Bonneil É, Caron-Lizotte O, Hardy MP, et al. Global
807 proteogenomic analysis of human MHC class I-associated peptides derived from non-
808 canonical reading frames. *Nat Commun.* 2016 Jan 5;7.
- 809 22. Ruiz Cuevas MV, Hardy MP, Hollý J, Bonneil É, Durette C, Courcelles M, et al. Most non-
810 canonical proteins uniquely populate the proteome or immunopeptidome. *Cell Rep.* 2021
811 Mar 9;34(10).
- 812 23. Scull KE, Pandey K, Ramarathinam SH, Purcell AW. Immunopeptidogenomics: Harnessing
813 RNA-Seq to illuminate the dark immunopeptidome. *Molecular and Cellular Proteomics.*
814 2021;20.
- 815 24. Zhao Q, Laverdure JP, Lanoix J, Durette C, Cote C, Bonneil E, et al. Proteogenomics uncovers a
816 vast repertoire of shared tumor-specific antigens in ovarian cancer. *Cancer Immunol Res.*
817 2020 Apr 1;8(4):544–55.
- 818 25. Laumont CM, Vincent K, Hesnard L, Audemard É, Bonneil É, Laverdure JP, et al. Noncoding
819 regions are the main source of targetable tumor-specific antigens. *Sci Transl Med.* 2018 Dec
820 5;10(470).
- 821 26. Ouspenskaia T, Law T, Clauser KR, Klaeger S, Sarkizova S, Aguet F, et al. Thousands of novel
822 unannotated proteins expand the MHC I immunopeptidome in cancer. Available from:
823 <https://doi.org/10.1101/2020.02.12.945840>
- 824 27. Chong C, Müller M, Pak H, Harnett D, Huber F, Grun D, et al. Integrated Proteogenomic Deep
825 Sequencing and Analytics Accurately Identify Non-Canonical Peptides in Tumor
826 Immunopeptidomes. Available from: <http://dx.doi.org/10.1101/758680>
- 827 28. Coulie PG, Lehmann F, Lethe B, Herman J, Lurquin C, Andrawiss M, et al. A mutated intron
828 sequence codes for an antigenic peptide recognized by cytolytic T lymphocytes on a human
829 melanoma. *Vol. 92, Immunology.* 1995.
- 830 29. Guilloux Y, Lucas S, Brichard VG, van Pel A, Viret C, de Plaen E, et al. A peptide recognized by
831 human cytolytic T lymphocytes on HLA-A2 melanomas is encoded by an intron sequence of
832 the N-acetylglucosaminyltransferase V gene. *Journal of Experimental Medicine.* 1996 Mar
833 1;183(3):1173–83.
- 834 30. Rong-Fu Wang B, Kawakami Y, Robbins PF, Rosenberg SA. Utilization of an Alternative Open
835 Reading Frame of a Normal Gene in Generating a Novel Human Cancer Antigen [Internet].
836 1996. Available from: <https://rupress.org/jem/article-pdf/183/3/1131/499993/1131.pdf>
- 837 31. Xiang H, Zhang L, Bu F, Guan X, Chen L, Zhang H, et al. A Novel Proteogenomic Integration
838 Strategy Expands the Breadth of Neo-Epitope Sources. *Cancers (Basel)* [Internet]. 2022 Jun
839 19;14(12):3016. Available from: <https://www.mdpi.com/2072-6694/14/12/3016>
- 840 32. Marcu A, Bichmann L, Kuchenbecker L, Kowalewski DJ, Freudenmann LK, Backert L, et al. HLA
841 Ligand Atlas: A benign reference of HLA-presented peptides to improve T-cell-based cancer
842 immunotherapy. *J Immunother Cancer.* 2021 Apr 15;9(4).

- 843 33. Ouspenskaia T, Law T, Clauser KR, Klaeger S, Sarkizova S, Aguet F, et al. Unannotated proteins
844 expand the MHC-I-restricted immunopeptidome in cancer. *Nat Biotechnol.* 2022 Feb
845 1;40(2):209–17.
- 846 34. Chong C, Müller M, Pak HS, Harnett D, Huber F, Grun D, et al. Integrated proteogenomic
847 deep sequencing and analytics accurately identify non-canonical peptides in tumor
848 immunopeptidomes. *Nat Commun.* 2020 Dec 1;11(1).
- 849 35. Kalaora S, Nagler A, Nejman D, Alon M, Barbolin C, Barnea E, et al. Identification of bacteria-
850 derived HLA-bound peptides in melanoma. *Nature.* 2021 Apr 1;592(7852):138–43.
- 851 36. Bassani-Sternberg M, Bräunlein E, Klar R, Engleitner T, Sinitcyn P, Audehm S, et al. Direct
852 identification of clinically relevant neoepitopes presented on native human melanoma tissue
853 by mass spectrometry. *Nat Commun.* 2016 Nov 21;7.
- 854 37. Newey A, Griffiths B, Michaux J, Pak HS, Stevenson BJ, Woolston A, et al.
855 Immunopeptidomics of colorectal cancer organoids reveals a sparse HLA class I neoantigen
856 landscape and no increase in neoantigens with interferon or MEK-inhibitor treatment. *J
857 Immunother Cancer.* 2019 Nov 18;7(1).
- 858 38. Kalaora S, Barnea E, Merhavi-Shoham E, Qutob N, Teer JK, Shimony N, et al. Use of HLA
859 peptidomics and whole exome sequencing to identify human immunogenic neo-antigens
860 [Internet]. Vol. 7. Available from: www.impactjournals.com/oncotarget
- 861 39. Cleyde J, Hardy MP, Minati R, Courcelles M, Durette C, Lanoix J, et al. Immunopeptidomic
862 analyses of colorectal cancers with and without microsatellite instability. *Molecular &
863 Cellular Proteomics* [Internet]. 2022 Apr;100228. Available from:
864 <https://linkinghub.elsevier.com/retrieve/pii/S1535947622000366>
- 865 40. Wang TY, Liu Q, Ren Y, Alam SK, Wang L, Zhu Z, et al. A pan-cancer transcriptome analysis of
866 exon splicing identifies novel cancer driver genes and neoepitopes. *Mol Cell.* 2021 May
867 20;81(10):2246-2260.e12.
- 868 41. Bartok O, Pataskar A, Nagel R, Laos M, Goldfarb E, Hayoun D, et al. Anti-tumour immunity
869 induces aberrant peptide presentation in melanoma. *Nature.* 2021 Feb 11;590(7845):332–7.
- 870 42. Bonté PE, Arribas YA, Merlotti A, Carrascal M, Zhang JV, Zueva E, et al. Single-cell RNA-seq-
871 based proteogenomics identifies glioblastoma-specific transposable elements encoding HLA-
872 I-presented peptides. *Cell Rep* [Internet]. 2022 Jun;39(10):110916. Available from:
873 <https://linkinghub.elsevier.com/retrieve/pii/S2211124722006933>
- 874 43. Nelde A, Flötotto L, Jürgens L, Szymik L, Hubert E, Bauer J, et al. Upstream open reading
875 frames regulate translation of cancer-associated transcripts and encode HLA-presented
876 immunogenic tumor antigens. *Cellular and Molecular Life Sciences.* 2022 Mar 1;79(3).
- 877 44. Mylonas R, Beer I, Iseli C, Chong C, Pak HS, Gfeller D, et al. Estimating the contribution of
878 proteasomal spliced peptides to the HLA-I ligandome. *Molecular and Cellular Proteomics.*
879 2018 Dec 1;17(12):2347–57.
- 880 45. Verkerk T, Koomen SJI, Fuchs KJ, Griffioen M, Spaapen RM. An unexplored angle: T cell
881 antigen discoveries reveal a marginal contribution of proteasome splicing to the

- 882 immunogenic MHC class I antigen pool. 2022; Available from:
883 <https://doi.org/10.1073/pnas.2119736119>
- 884 46. Poschke IC, Hassel JC, Rodriguez-Ehrenfried A, Lindner KAM, Heras-Murillo I, Appel LM, et al.
885 The Outcome of Ex Vivo TIL Expansion Is Highly Influenced by Spatial Heterogeneity of the
886 Tumor T-Cell Repertoire and Differences in Intrinsic in Vitro Growth Capacity between T-Cell
887 Clones. *Clinical Cancer Research*. 2020 Aug 15;26(16):4289–301.
- 888 47. Dersh D, Hollý J, Yewdell JW. A few good peptides: MHC class I-based cancer
889 immunosurveillance and immunoevasion. Vol. 21, *Nature Reviews Immunology*. Nature
890 Research; 2021. p. 116–28.
- 891 48. Yewdell JW. DRiPs solidify: Progress in understanding endogenous MHC class I antigen
892 processing. Vol. 32, *Trends in Immunology*. 2011. p. 548–58.
- 893 49. Norbury CC, Basta S, Donohue KB, Tschärke DC, Princiotta MF, Berglund P, et al. CD8 + T Cell
894 Cross-Priming via Transfer of Proteasome Substrates. Vol. 304, *New Series*. 2004.
- 895 50. Gros A, Parkhurst MR, Tran E, Pasetto A, Robbins PF, Ilyas S, et al. Prospective identification
896 of neoantigen-specific lymphocytes in the peripheral blood of melanoma patients. *Nat Med*.
897 2016 Apr 1;22(4):433–8.
- 898 51. Cohen CJ, Zhao Y, Zheng Z, Rosenberg SA, Morgan RA. Enhanced antitumor activity of
899 murine-human hybrid T-cell receptor (TCR) in human lymphocytes is associated with
900 improved pairing and TCR/CD3 stability. *Cancer Res*. 2006 Sep 1;66(17):8878–86.
- 901 52. Cohen CJ, Li YF, El-Gamil M, Robbins PF, Rosenberg SA, Morgan RA. Enhanced antitumor
902 activity of T cells engineered to express T-cell receptors with a second disulfide bond. *Cancer*
903 *Res*. 2007 Apr 15;67(8):3898–903.
- 904 53. Haga-Friedman A, Horovitz-Fried M, Cohen CJ. Incorporation of Transmembrane
905 Hydrophobic Mutations in the TCR Enhance Its Surface Expression and T Cell Functional
906 Avidity. *The Journal of Immunology*. 2012 Jun 1;188(11):5538–46.
- 907 54. Chong C, Marino F, Pak H, Racle J, Daniel RT, Müller M, et al. High-throughput and sensitive
908 immunopeptidomics platform reveals profound interferon γ -mediated remodeling of the
909 human leukocyte antigen (HLA) ligandome. *Molecular and Cellular Proteomics*. 2018 Mar
910 1;17(3):533–48.
- 911 55. Marcu A, Bichmann L, Kuchenbecker L, Backert L, Kowalewski DJ, Freudenmann LK, et al. The
912 HLA Ligand Atlas. A resource of natural HLA ligands presented on benign tissues. Available
913 from: <http://dx.doi.org/10.1101/778944>
- 914
- 915
- 916
- 917

918 **Figures**

- 919 Figure 1. Identification and characteristics of non-canonical HLA-I ligands presented by patient-derived
920 tumor cell lines
921 Figure 2. Candidate tumor antigens presented on HLA-I from patient-derived TCL identified through
922 proteogenomics.
923 Figure 3. Pre-existing T-cell responses to candidate tumor antigens in cancer patients.
924 Figure 4. *In vitro* sensitization of donor PBLs identified three nonC-TL shared across patient-derived TCLs.
925 Figure 5. Evaluation of the tumor specificity of the three immunogenic nonC-TL.

926 **Tables**

- 927 Table 1. Immunogenic tumor antigens identified in cancer patients.

928 **Supplemental Figures and tables**

- 929 Supplemental Figure 1. Validation of HLA-I ligand tumor antigen candidates with synthetic peptides.
930 Supplemental Figure 2. Validation of selected HLA-I ligand tumor antigen candidates identified in Mel-1 and
931 Mel-3 with isotope-labeled peptides.
932 Supplemental Figure 3. Frequency of nonC peptides detected in HLA-I.
933 Supplemental Figure 4. HLA-I allele binding motif of all patients included in the study.
934 Supplemental Figure 5. A fraction of nonC-TL can be detected in publicly available immunopeptidomics
935 datasets from human tumor biopsies.
936 Supplemental Figure 6. Evaluation of pre-existing T-cell responses to candidate tumor antigens in cancer
937 patients.
938 Supplemental Figure 7. Enrichment of antigen-specific T cells from cancer patients by flow cytometry-based
939 sorting.
940 Supplemental Figure 8. Deconvolution of peptide pools containing recognized CGA or melanoma-associated
941 antigens.
942 Supplemental Figure 9. Functional avidity and specificity of neoantigen-specific T cells isolated from cancer
943 patients.
944 Supplemental Figure 10. HLA restriction element and recognition of autologous tumor cell lines by antigen-
945 specific T cells isolated from cancer patients.
946 Supplemental Figure 11. Genomic location of the three immunogenic nonC-TL identified through IVS.
947 Supplemental Figure 12. Recognition of the predicted ORFs encoding the immunogenic nonC-TL by TCR
948 transduced cells.
949 Supplemental Figure 13. Loss of recognition of TCL transfected with Cas9-sgRNA targeting the predicted
950 5'U-HOXC13 ORF.
951 Supplemental Figure 14. Assessment of expression and translation of the immunogenic nonC-TL in human
952 healthy cells.
953 Supplemental Figure 15. NonC-TL are the main source of candidate tumor antigens identified by
954 proteogenomics but tumor-reactive T cells preferentially recognize neoantigens derived from NSM.
955 Supplemental Table 1. Patient characteristics and relevant experimental information.

956 **Supplemental data**

- 957 Supplemental Data 1. HLA-I typing of tumor cell lines.
958 Supplemental Data 2. MS information HLA-I ligands $FDR \leq 0.01$ and $ALC \geq 30$.
959 Supplemental Data 3. HLA-I ligands derived from NSM.

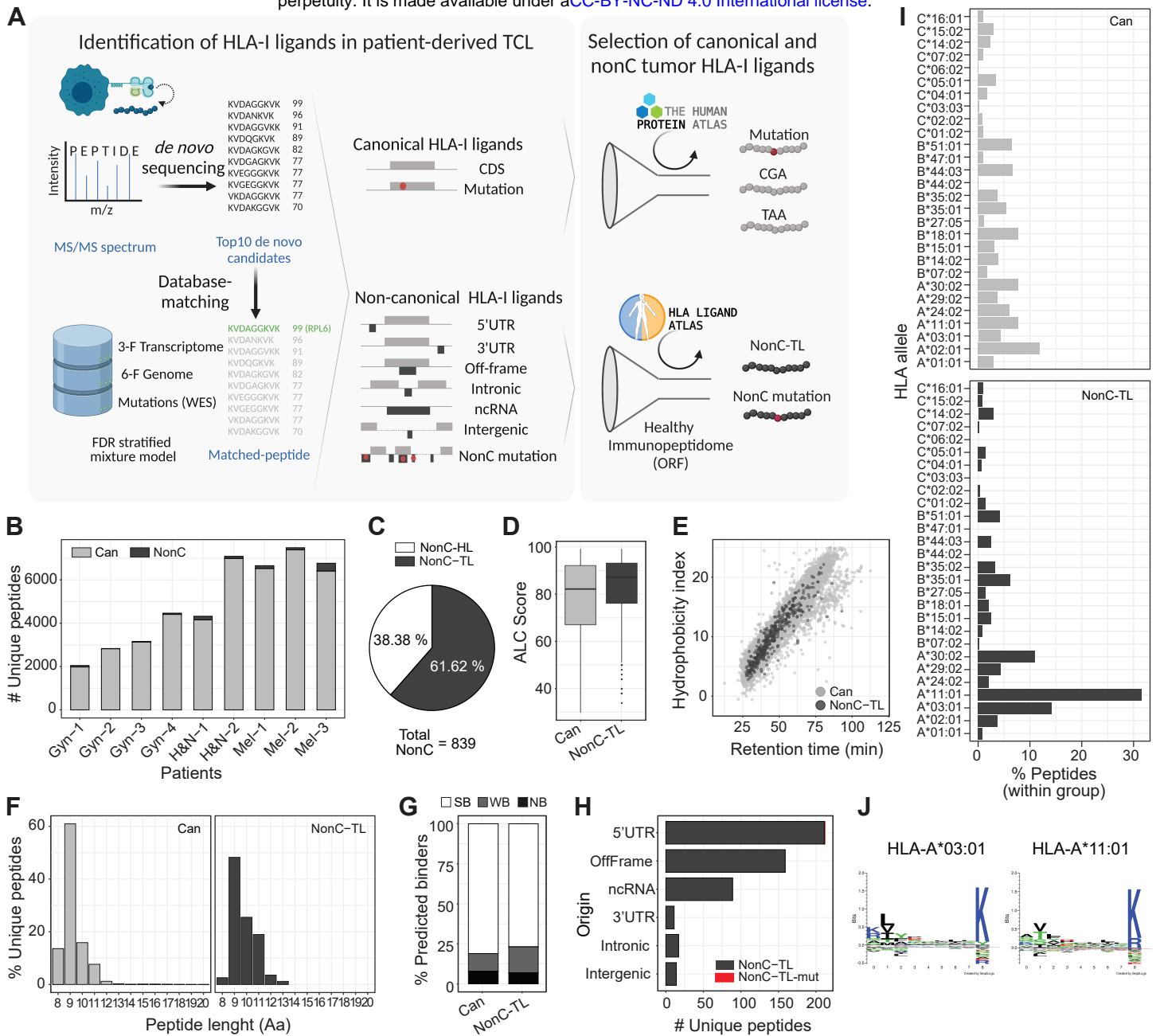


Figure 1. Identification and characteristics of non-canonical HLA-I ligands presented by patient-derived tumor cell lines. (A) Diagram depicting the pipeline used to identify HLA-I ligands derived from canonical (Can) and non-canonical (nonC) proteins presented by patient-derived TCL. The Top10 candidates for each MS spectrum were identified by de novo sequencing and aligned to a database containing the 3-frame transcriptome, 6-frame genome and the NSM identified by WES. The FDR was calculated for each category shown using a stratified mixture model (left panel). All canonical peptides containing mutations as well as peptides derived from CGA or TAA were further studied. For nonC HLA-I ligands, healthy immunopeptidomics data from HLA ligand atlas was used to filter out peptides presented in healthy tissues at the ORF level to obtain the nonC-TL (right panel). Image created with BioRender. (B) Number of canonical and non-canonical HLA-I peptides identified per patient. (C) Percentage of nonC peptides derived from predicted ORF present or absent in a healthy tissue immunopeptidome data set (nonC-HL and nonC-TL, respectively). (D) ALC identification score of canonical and nonC-TL. (E) Predicted hydrophobicity index (y axis) and retention time (x axis). Each dot represents a unique peptide sequence. (F) Length distribution of unique HLA-I peptide sequences. Only peptides <20 Aa are depicted. (G) Percentage of peptides predicted to bind to the patient specific HLA alleles according to NetMHCpan4.0. Peptides were categorized into strong binders (SB; %-tile rank ≤ 0.5), weak binders (WB; %-tile rank = 0.5-2) or non-binders (NB; %-tile rank > 2). (H) Number of nonC-TL originated from each of the ORF categories noted. (I) HLA allele binding preference of Can and nonC-TL. For each peptide, only the min rank predicted by NetMHCpan4.0 was considered. (J) Consensus peptide binding motif of the two HLAs predicted to present the majority of the nonC peptides identified. Image downloaded from NetMHCpan4.0 motif viewer. In all the analyses shown, the FDR threshold was set at 0.01 and ALC identified at 30.

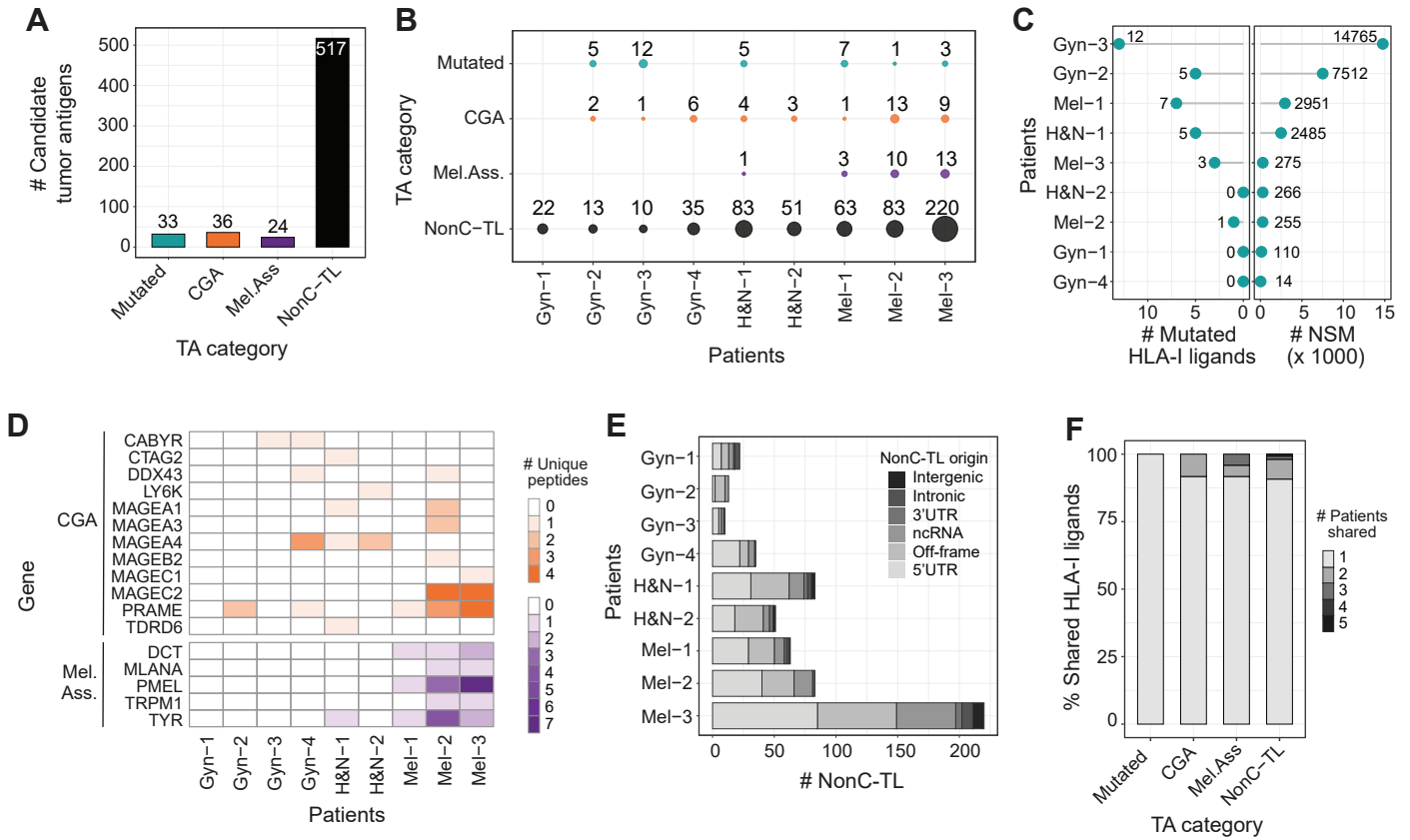


Figure 2. Candidate tumor antigens presented on HLA-I from patient-derived TCL identified through proteogenomics. (A) Total number of unique peptide sequences derived from candidate tumor antigens (TA) by category. Data from all patients was pooled together. Only unique peptide sequences were considered. (B) The number and category of TA are displayed for each TCL. (C) The number of mutated peptides eluted from HLA-I (left) and number of NSM identified by WES (right) are displayed for each patient. (D) Heat map displaying the number of epitopes derived from specific CGA or melanoma-associated antigens per patient. (E) Number of nonC-TL originated from each ORF category per patient. (F) Percentage of candidate TA uniquely identified in one patient or shared by TA category. The FDR threshold was set at 0.02 for mutations and 0.01 for all other categories.

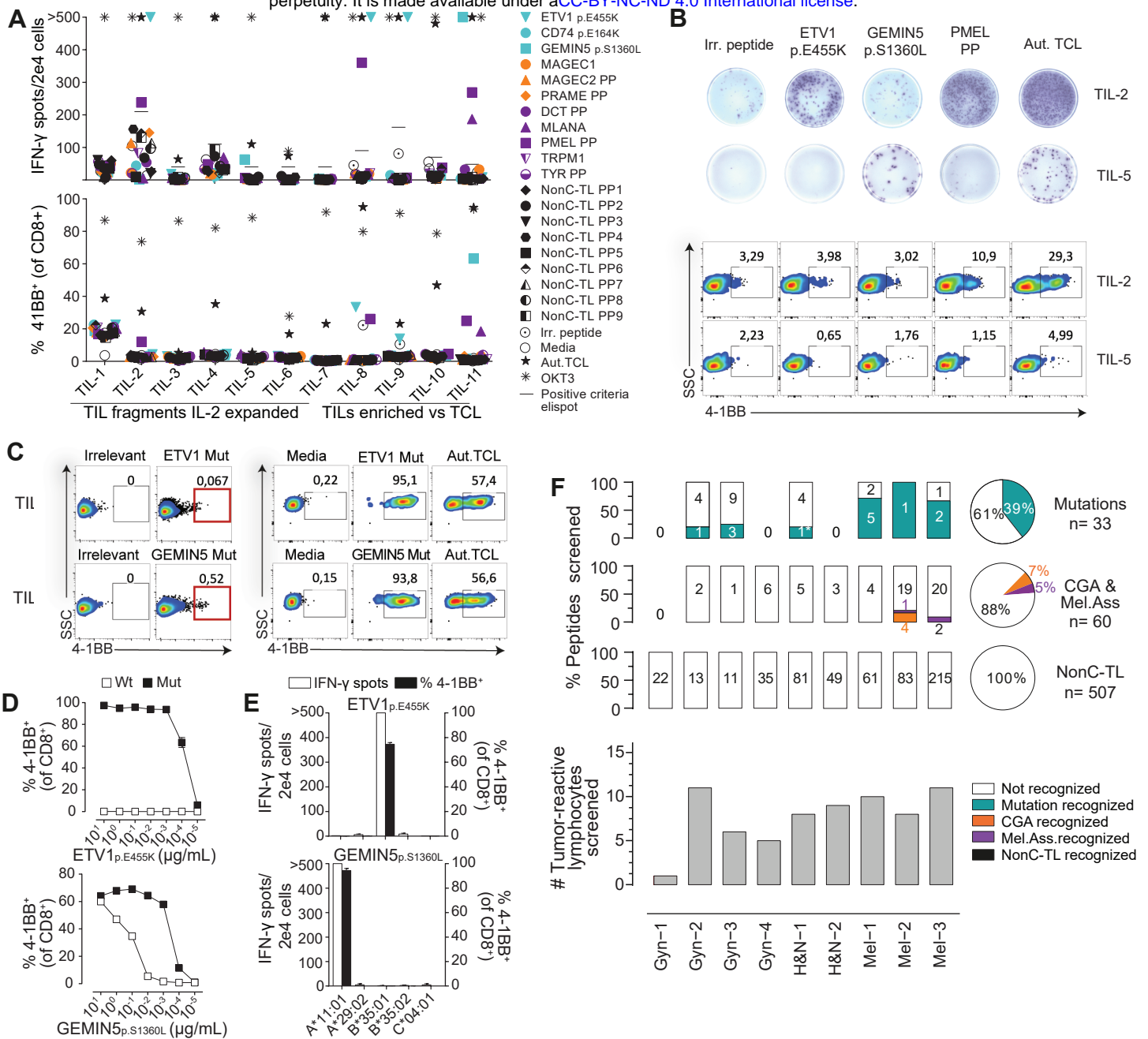


Figure 3. Pre-existing T-cell responses to candidate tumor antigens in cancer patients.

For each patient, reactivity was evaluated by co-incubating 2e4 T cells (TIL or PBL sorted based on specific markers, e.g., PD1^{hi}), with 2e5 autologous APC pulsed with 1 μ g/mL of selected peptides either alone or in pools (PP). IFN- γ ELISPOT and 4-1BB upregulation by FACS were used to measure T-cell responses after 20 h. **(A)** Reactivity to tumor antigen candidates for Mel-3. The number of IFN- γ spots per well (top panel) and the percentage of cells expressing 4-1BB (bottom panel) are shown. Mutated peptides are plotted in turquoise, CGA in orange, melanoma-associated in purple, and nonC-TL in black. PP, peptide pool. **(B)** Representative ELISPOT results (top) and flow cytometry plots (bottom) for TIL-2 and TIL-5 from Mel-3 with the targets specified. **(C)** TIL populations recognizing the mutated HLA-I peptides indicated were enriched by flow cytometry sorting of 4-1BB⁺ lymphocytes and expanded for 14 days. Plot showing gates used for sorting (left) and recognition of the targets specified after expansion (right). **(D)** T cell reactivity of neoantigen-enriched T-cell populations to serial dilutions of the wild type (Wt) or mutant (Mut) ETV1_{p.E455K} and GEMIN5_{p.S1360L} peptides. **(E)** Neoantigen-enriched population were co-cultured with COS-7 cells transfected with the indicated individual HLA-I alleles and pulsed with the corresponding peptides to determine the restriction element. **(F)** Summary of the reactivity against candidate tumor antigens in all patients studied. The percentage and the absolute number of recognized and non-recognized peptides within each category are shown per patient (bar plot) and for all the patients studied (pie chart). The number of tumor-reactive lymphocytes tested for each patient is shown on the bottom. Plotted cells were gated on live CD3⁺CD8⁺ lymphocytes. '>' denotes greater than 500 spots/2e4 cells. *Mutation recognized previously identified. Experiments were performed twice.

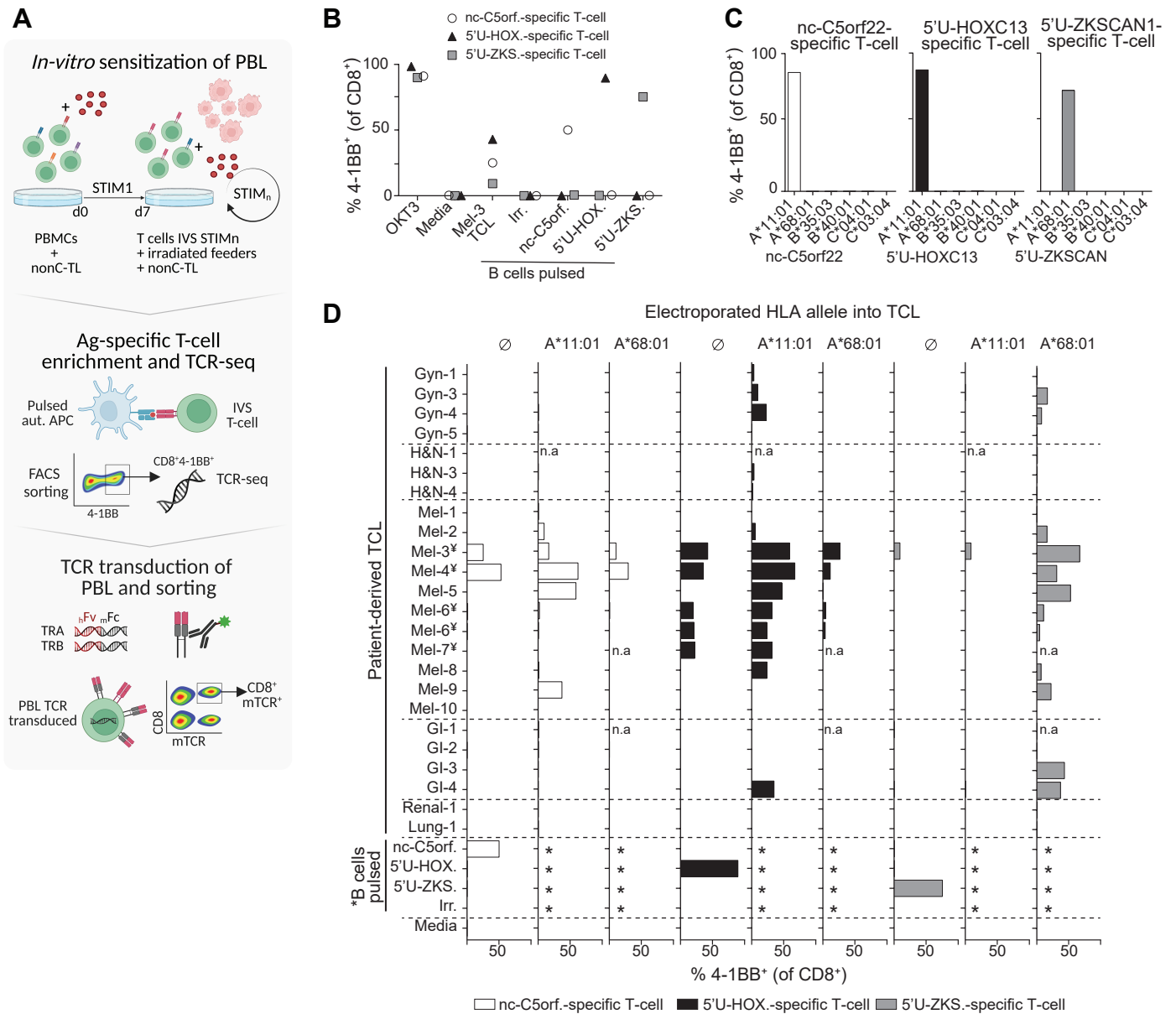


Figure 4. *In vitro* sensitization of donor PBL identified three immunogenic nonC-TL shared across patient-derived TCLs. (A) Donor PBL were *in vitro* sensitized (IVS) via three consecutive rounds of stimulation with 170 selected nonC-TL predicted to bind to HLA-A*11:01. Reactive T cells were enriched through FACS sorting based on CD8⁺ 4-1BB⁺ expression after 20 h co-culture with autologous B cells pulsed with the specific peptides and expanded for 14 days. The top 1 αβ pairs were cloned into a retroviral vector to transduce PBL and CD8⁺ mTCR⁺ cells were FACS sorted to obtain a pure transduced population. Image created with BioRender. (B) Reactivity of antigen-specific T cells generated by IVS following FACS sorting enrichment. Frequency of 4-1BB⁺ on CD8⁺ cells after 20 h co-culture with B cells pulsed with the HPLC peptides specified is depicted. (C) Restriction element was evaluated by co-culturing enriched T-cell populations with COS-7 cells expressing the donor HLA alleles and pulsed with the corresponding peptides. (D) Expression and translation of the immunogenic nonC-TL in multiple patient-derived TCL indirectly evaluated through the detection of 4-1BB expression of nonC antigen-specific T cells co-cultured with TCL left untreated or electroporated with RNA encoding the specified HLA-I alleles. *B cells were not electroporated. ‡TCL naturally expressing HLA-A*11:01. n.a, non-assessed.

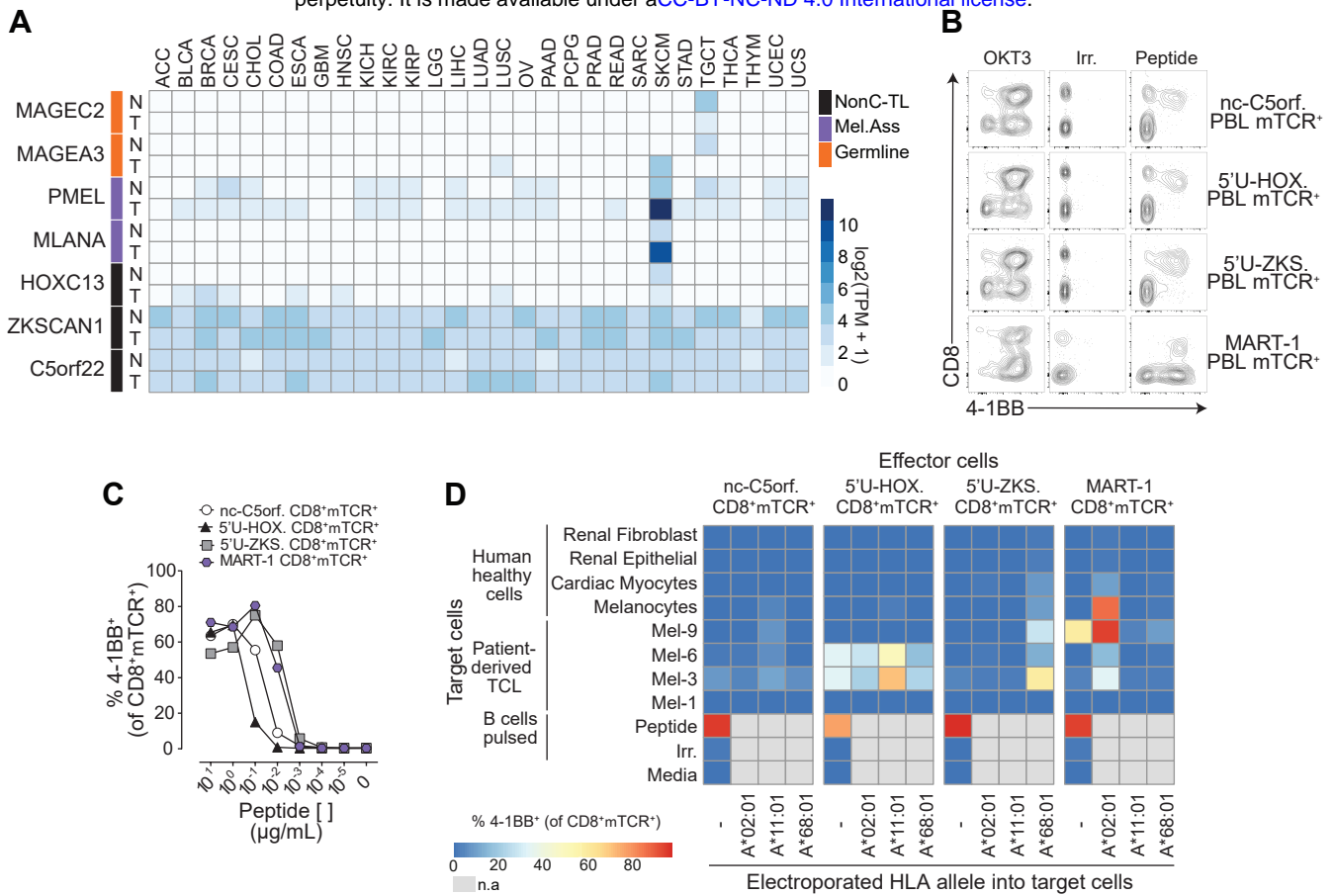


Figure 5. Evaluation of the tumor specificity of the three immunogenic nonC-TL.

(A) RNA expression analysis in tumors (T) and matched healthy tissues (N) of the canonical genes encoding immunogenic nonC-TL compared to TAA and CGA. TCGA and GTEX data were obtained from GEPIA. (B) CD8 coreceptor activation-dependence of PBL transduced with antigen-specific TCRs. FACS plots show the expression of 4-1BB by CD8 (gated on CD3⁺mTCR⁺) after co-culture with peptide pulsed B cells. B cells pulsed with an irrelevant (Irr.) peptide were used as negative control. (C) TCR-transduced T cells purified by FACS sorting (CD8⁺mTCR⁺) were co-cultured with B cells pulsed with serial dilutions of the corresponding peptide. SD mean is plotted. (D) Expression and translation of nonC-TL in healthy human cells and selected TCLs was indirectly evaluated by co-culturing control and electroporated target cells with RNA encoding the specified HLA alleles with sort purified TCR-transduced T cells. T-cell activation was assessed by measuring 4-1BB expression on CD8⁺mTCR⁺. n.a., non-assessed.

Table 1. Immunogenic tumor antigens identified in cancer patients

Patients	TA ^a	Gene ^b	Sequence ^c	Predicted	Predicted	Restriction
				HLA allele ^d	binder (min rank) ^e	
Gyn-1		KIF2C _{p.L175F}	IPSKC F LLV	B*51:01	SB (0.3137)	n.a
		FUBP1 _{p.R365Q}	IITDLL Q SV	A*02:01	SB (0.1403)	A*02:01
Gyn-2		LAMB3 _{p.D710A}	A PSGAFRML	B*07:02	SB (0.0203)	B*07:02
		RPL19 _{p.I137V}	V LMEHIHKL	A*02:01	SB (0.0034)	A*02:01
H&N-1		RPL14 _{p.H20Y}	GP Y AGKLVAI	B*07:02	SB (0.1369)	B*07:02
Mel-1		CDKN2a _{p.G74fs}	A VCP W T W L R	A*11:01	SB (0.3405)	A*11:01
		DUSP3 _{p.S81F}	FYKD F GITY	C*14:02	SB (0.0137)	C*14:02
		NAT10 _{p.A320V}	A VIPLPLVK	A*11:01	SB (0.0057)	A*11:01
		SRRT _{p.A434V}	IAPNIS R V	B*51:01	WB (0.5504)	B*51:01
		TRRAP _{p.S2502F}	AML P FITNV	A*02:01	SB (0.0092)	A*02:01
Mel-2		MAGEA6 _{p.E168K}	K VDPIGHVY	A*30:02	SB (0.0045)	A*30:02
		MAGEA3	EVDPIGHLY	A*01:01	SB (0.0039)	n.a
		MAGEA3	MEVDPIGHLY	B*18:01	SB (0.0055)	n.a
		MAGEB2	KVNPNGHTY	A*30:02	SB (0.0032)	n.a
		MAGEC2	GVYAGREHFVY	A*30:02	WB (0.5942)	n.a
		TYR	HEAPAFLPW	B*18:01	SB (0.0488)	B*18:01
Mel-3		ETV1 _{p.E455K}	HPYN K GYVY	B*35:01	SB (0.0043)	B*35:01
		GEMIN5 _{p.S1360L}	STFKEL F LEK	A*11:01	SB (0.0295)	A*11:01
		MLANA	MPREDAHF	B*35:01	SB (0.4758)	n.a
		PMEL	GTATLRLVK	A*11:01	SB (0.0531)	n.a

Table 1. Immunogenic tumor antigens identified in cancer patients. ^aThe category of the tumor antigen (TA) is depicted in colors; mutated in turquoise, cancer-germline in orange and melanoma-associated in purple. ^bGene symbol, the amino acid change and position in the protein are shown. ^cMutated amino acids are highlighted in red letters. ^{d,e}HLA predicted binding affinity using NetMHCpan4.0, only the allele with the minimal rank is shown. SB: Strong binders (%-tile rank ≤2); NB: non-binders (%-tile rank >2). ^fRestriction element was evaluated experimentally by co-incubating reactive lymphocytes with COS-7 cells transfected with plasmids encoding for the individual HLA followed by peptide pulsing. T-cell responses were measured by IFN γ elispot and 4-1BB upregulation. n.a=non-assessed